ARTICLE TEMPLATE

A co-simulation model of building-integrated urban farms to quantify synergistic benefits of different coupled configurations

Melanie Jans-Singh[a], Rebecca Ward[a,b] and Ruchi Choudhary[a,b]

[a]Engineering Department, University of Cambridge, Cambridge, UK; [b]Alan Turing Institute, London, UK

ARTICLE HISTORY
Compiled March 18, 2021

ABSTRACT
Recent findings suggest that rooftop greenhouses could be more efficient when combined with waste streams in buildings, but there is a gap in quantification of the combined performance of building integrated greenhouses. This paper addresses this deficit for school buildings in London, UK, where urban agriculture is of increasing interest. A building energy simulation (BES) of an archetype school building is developed in EnergyPlus and co-simulated with a validated greenhouse energy simulator (GES). The performance of different greenhouse-building coupling configurations is evaluated to estimate the potential for crop growth, heat recovery and reduction in ventilation demand, through a sensitivity analysis and parametric study. Our results show that a 250 m^2 greenhouse on the top floor of the school could produce 6t lettuce with half the energy demand of the same standalone greenhouse. Trade-offs across increase in humidity, yields, and energy efficiency indicate the importance of modelling to ensure optimal designs.

KEYWORDS
co-simulation; building integrated agriculture; greenhouse modelling; urban agriculture

1. Introduction

Urban greenhouses could have higher efficiency and multiple benefits in cities when designed in symbiosis with the surrounding urban environment; an attractive solution to growing concerns of cities' environmental impacts. Population growth, land erosion, and rapid urbanisation are increasing pressure on local councils and businesses to provide energy, water, transport and food security for the city dwellers. By 2050, 3.5 billion more people will inhabit this planet, 2.6 billion of which are predicted to be living in cities (United Nations 2019). Hunter et al. (2017) shows that food demand will rise by around 30%, outpacing increases in arable land. At the same time, with increased globalised trade, countries are rarely self-sufficient. Instead complex supply and transport systems govern how food arrives in our plates. In the UK, fruit and vegetables are by far the largest source of imports representing 37% of the UK's total food trade gap. This amount has been growing as the cultivated area of fruit and vegetables is following a declining trend, with a 27% decrease since the 1980s (Schoen and Lang 2016). In addition, global food production accounts for 26% of anthropogenic greenhouse gas

CONTACT Melanie Jans-Singh. Email: mkj32@cam.ac.uk

emissions (Poore and Nemecek 2018). It is also a resource intensive industry, using 50% of habitable land (Roser and Ritchie 2019) and 70% of the world's freshwater resources for irrigation (Fischer et al. 2007). Although a large proportion of the environmental footprint of agriculture comes from meat and grain production (Poore and Nemecek 2018), greenhouses offer a potential for more resource-efficient cultivation, while also reducing the risk of flooding, soil erosion, acidification and eutrophication of waters caused by conventional agriculture (Kulak, Graves, and Chatterton 2013), thereby allowing to sustain functioning ecosystems at multiple scales.

Urban agriculture is already prevalent around the world, with 100 million people engaged in the production and/or commercialisation of urban produce (Orsini et al. 2013). Existent systems range from simple edible roof gardens, to advanced plant factories (Kozai 2016) and building integrated agriculture (BIA) (Sanyé-Mengual et al. 2015). Goldstein et al. (2016) describe a "renaissance of urban agriculture in the world's wealthy, northern cities" as new technologies like hydroponics, with their significantly higher yields and water recycling ratio per square metre, offer the promise of competing with traditional agriculture. However, the benefits of reduced food miles may be outweighed by the energy inputs and inefficient use of production outputs. Over the past decade, research into urban agriculture has developed considerably: from socio-economic analyses (Specht et al. 2013), and speculative futuristic ideas (Despommier 2011), to cost-benefit comparisons of alternatives for reusing roofs in cities (Benis et al. 2018). These studies highlight the need to exploit available resources with the surrounding built environment synergistically when designing BIA to reduce energy inputs for heating, lighting, water, and ventilation requirements.

Nadal et al. (2017), for example, show that the potentially high energy cost of hydroponic rooftop greenhouses could be offset by exploiting the symbiotic relationship between a greenhouse and the waste resources present in the host building in the form of heated CO_2 rich air and rain water. However, the interchange of air between a building and a greenhouse is only possible if the impact of plants on indoor environment is quantified in terms of temperature, humidity, and CO_2 levels. Experimental studies that observe the carbon sequestration and water vapour loss of houseplants have demonstrated the cooling effect that plants can have on the indoor environments (Gubb et al. 2018). A number of established models exist to simulate the photosynthesis (Vanthoor 2011; Farquhar, von Caemmerer, and Berry 1980) and transpiration of crops (Jolliet and Bailey 1992; Stanghellini and van Meurs 1992; Boulard et al. 2017), which have led to complex greenhouse environment models for commercial greenhouses (Graamans et al. 2017). However, the interdisciplinary integration of the separate domains of plant models and Building Energy Simulation (BES) models remains challenging.

Previous work on modelling Building Integrated Agriculture (BIA) have so far either simplified the effect of transpiration, omitted plants completely, or externally linked with transpiration and crop growth models, thus omitting the feedback between plants and the indoor built environment. For example, rooftop greenhouses have been modelled in combination with EnergyPlus in the following cases: Léveillé-Guillemette and Monfet (2016) evaluated different heating configurations for a rooftop solar greenhouse in Canada, but they did not include the effects of plants, thus omitting the addition of moisture in the environment. Benis, Reinhart, and Ferrao (2017) and Nadal et al. (2017) developed a rooftop greenhouse model for Mediterranean climates, but represented humidity and temperature change of the greenhouse through proxy equations. Benis, Reinhart, and Ferrao (2017) used EnergyPlus to calculate temperature and humidity as inputs for Vanthoor (2011)'s greenhouse model, which estimates the resulting

crop production. Transpiration was represented in the BES through an evaporative cooling pad with pre-determined load. The "living lab" rooftop greenhouse in the ICTA building in Barcelona was also modelled with EnergyPlus (Nadal et al. 2017; Muñoz-Liesa et al. 2020). However, because the model focuses on the exchange of the warm air from the building to the rooftop greenhouse and vice versa, the transpiration was simplified to a function of the day of the year through a system variable, and had negligible effects. However, the further study on this building by Muñoz-Liesa et al. (2020) found that transpiration of plants needed improved modelling as it may have repercussions on air-conditioning demand. There is currently no complete simulation methodology to quantify and optimise the integration of a greenhouse with a building as a thermodynamic element. This is an important gap in the current literature, as it is the only mechanism to optimally design the reuse of available building resources (waste heat and CO_2 from buildings for example), while also understanding the impact that the greenhouse would have on the indoor air quality of the building.

BIA is still in its infancy due to its uncertain financial and environmental cost/benefits, but the precedent for integrating greenhouses in schools is increasing. This is likely due to burgeoning social movements, and the promotion of health and wellbeing impacts of growing plants (Siegner, Sowerwine, and Acey 2018). Three out of four schools in London have allotments upon which they run educational programmes to support the teaching of science, maths and environment studies (Capital Growth 2016). Schools are increasingly using greenhouses as green classrooms (Thomaier et al. 2015), especially in primary and secondary schools (Nadal et al. 2018). The Greenhouse Project in New York has, as shown in Figure 1 for example, built 86 labs containing hydroponic greenhouses on school roofs and old classrooms "to educate students and teachers about the science of sustainability" (New York Sun Works 2020). However, Nadal et al. (2018) points out that good governance and knowledge of the potential benefits of BIA in schools need to be better defined to encourage further uptake of BIA.

Figure 1. Rooftop greenhouse on school in New York (New York Sun Works 2020)

This paper seeks to address these research gaps by presenting a unique co-simulation

methodology that couples a Greenhouse Energy Simulation (GES) and a Building Energy Simulation (BES), with the aim to support the design and optimisation of BIA. Given the appetite for food growing in schools, this methodology is tested on an archetype of a secondary school in London. Building on Jans-Singh, Ward, and Choudhary (2020) where this co-simulation concept was first introduced, the in-depth analysis and presentation of the co-simulation methodology in this paper provides the following two new contributions. (i) Identification of the effects of integrating a greenhouse on the heat and mass balance of the zone of interest, and (ii) Understanding of the influence of the design and operational parameters through a sensitivity analysis and parametric study.

The structure of the paper is as follows. The first two sections present the development of the two models respectively: in Section 2, we develop a plausible BES model of an archetype of a secondary school in London with a greenhouse on the top floor. Section 3 presents a summary of the Greenhouse Energy Simulation (GES), with details provided in the appendix. The original GES model was validated for ornamental greenhouses (Ward and Choudhary 2014), and later adapted to model an underground farm in London (Ward, Jans-Singh, and Choudhary 2018). As such, GES was designed to model plant transpiration and photosynthesis, but not crop yield. For the purpose of this study, the GES model is extended to represent a BIA greenhouse growing lettuce year-round hydroponically following Von Caemmerer (2013) and Farquhar, von Caemmerer, and Berry (1980) including a harvesting element, and adapted to use inputs from a BES model. This model, which can now be applied to a BIA in any context with a horizontal hydroponic system, is hitherto referred to as GES-II. Section 4 presents the co-simulation methodology, which includes the strategy for linking the two models as well as the use of a sensitivity analysis to identify the key input parameters for selected quantities of interest. Results are presented in Section 5. This includes the analysis of the co-simulation outputs. In addition, the sensitivity analysis is used to quantify the relative influence of design parameters on the performance of the building integrated greenhouse with respect to energy use and crop yields. The simulation runs for the SA are used for a parametric study to evaluate different design configurations in relation to the model outcomes.

2. Energy model of an archetype school building in London (BES)

The BES model is created for a building archetype of school building in London by analysing building stock data, national guidelines and statistics. The energy use intensity of school buildings is plotted against the school headcount in Figure 2, illustrating the relative consumption of state-funded secondary schools compared with the other tree main types of schools in Greater London: state funded primary, special needs schools, and independent schools. The dataset has been collated from the 2018 National Statistics for schools from the UK Department for Education (DfE 2018) and Display Energy Certificates (DEC) (DCLG 2020). Due to the larger headcount and building surface area, it was decided to build the model for secondary schools. As shown with the purple lines in Figure 2, their average reported energy use intensity (EUI) is 172.6 ± 47.6 kWh/m^2/year, with 64.4 and 116 kWh/m^2 for electricity and thermal EUI respectively. Average headcounts are 1036 students. Best practice EUI (25th percentile[1]) for electricity and thermal energy were 50 and 90 kWh/m^2 . Results

[1]The 25th percentile was chosen to represent best practice, following Hong (2015)'s thesis titled *Benchmarking the energy performance of the UK non-domestic stock: a schools case study.*

were in line with Dias Pereira et al. (2014)'s study, which found UK secondary schools typically consume 177 kWh/m^2, with best practice consumption of 133 kWh/m^2. The dataset also reveals that although all secondary schools are heated, only 25% are mechanically ventilated, and 60% have some form of air-conditioning. The energy rating (DEC band) was in general poorer for secondary schools (33% have an E rating) than primary schools (for which the most common is the D rating). On average, the London secondary schools were inspected 4.2 times between 2008 and 2019, which noticed an average energy improvement of 22.4 kWh/m^2, which suggests there is potential for consideration of further energy saving measures. Following these statistics, the school building is designed for 900 students, with a target best practice energy consumption of ca. 135 kWh/m^2.

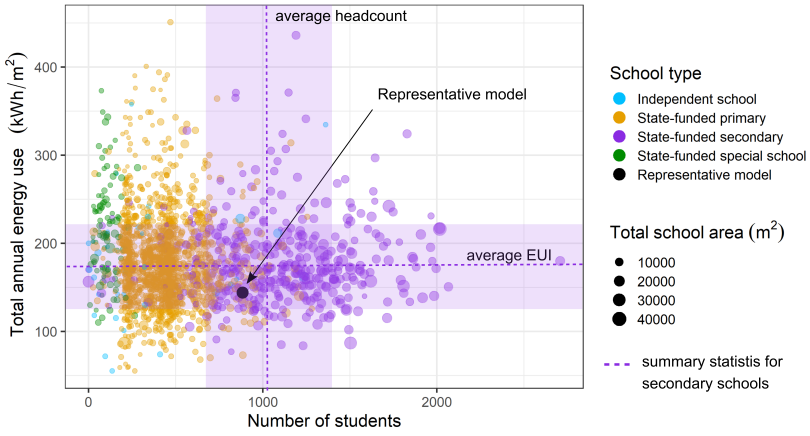

Figure 2. Energy Use Intensity (thermal and electrical) of the 3309 schools in Central London, plotted against headcount of students. Data from combined DEC certificates and National Statistics for Schools merged by postcode. The black point shows where the representative model situates itself. The mean (dotted line) and standard deviation (purple band) for secondary schools are represented with purple lines.

2.1. *Building configuration*

The physical configuration of the archetype school is based on DfE (2014) which stipulates area guidelines for schools, and is illustrated in Figure 3. The secondary school is designed for 900 students, and accordingly has a floor area of 7428 m^2 (without greenhouse), based on Tian and Choudhary (2012). The building has three storeys, to match the average building height of 10 to 14 m for school buildings in London found from a commercial land use and building type database (The GeoInformation Group 2017). The school is comprised of 53 zones, organised by orientation, floor and usage type. The usage types are: classrooms (teaching and learning areas), circulation (hallways and entrance), staff rooms, cafeteria, storage, toilets, and gym. In addition, this school building model contains a "Greenhouse Zone" (GZ) of 252 m^2 on the top floor, in the South facing direction, above a classroom zone, bringing the total floor area to 7680 m^2.

Building fabric and materials are specified as per the National Calculation Methodology (BRE 2016). Tian and Choudhary (2012) found that roof U-value, infiltration, heating set-point and ventilation are the most sensitive parameters of the energy model for school buildings in London. The guidelines stipulates a U-value of 0.26 W/m^2 K for exterior walls, and 0.18 W/m^2 K for the roof (BRE 2016). To account for older buildings representing the London building stock, the U-values chosen to be representative

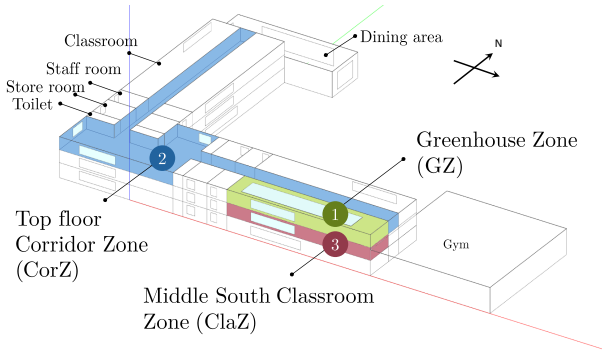

Figure 3. Representation of the school building model, with the three zones of interest: (1) the Greenhouse Zone (GZ), (2) the top floor Corridor Zone (CorZ), and (3) the south facing Classroom Zone on the middle floor (ClaZ).

are $0.68\,\mathrm{W/m^2\,K}$ for the exterior wall and $0.55\,\mathrm{W/m^2\,K}$ for the roof. The infiltration is a DOE-2 model as it includes the likely higher infiltration rate on the top floor (Gowri, Winiarski, and Jarnagin 2009), with a rate of 0.3 air changes per hour (ACH) to reflect the likely slight deviation from the guideline requirement of $3\,\mathrm{m^3/m^2\,h}$ (DES 2019). As this is a demonstration example of the co-simulation methodology, the building materials and infiltration rate for the GZ are the same as for the rest of the building. In its baseline design, the GZ also harbours a large roof window of 70% of the floor area, which brings an average Daily Light Integral (DLI) of $10.35\,\mathrm{mol/m^2/day}$ to a cultivated area of 50% of the floor area over the year. Reducing the window to 50% or increasing to 90% of the floor area would respectively yield a DLI of 7.57 and $13.21\,\mathrm{mol/m^2/day}$ (averaged over the year)[2]. These numbers show that this greenhouse has the potential to be within the target range of the environmental PAR integral of $11\,\mathrm{mol/m^2/day}$ to $17\,\mathrm{mol/m^2/day}$ recommended for greenhouse lettuce by Ferentinos, Albright, and Ramani (2000) for significant parts of the year. As such, it is possible that CO_2 enrichment will be cost-effective (Both, Albright, and Langhans 1998). The effect of modifying the window size or cultivated area on seasonal and annual crop growth and energy demand will be investigated in Section 5.

2.2. *Operational parameters for zones of interest*

Three zones of the school are relevant for modelling the coupling between the greenhouse and the school building, in order to quantify the potential of reusing "waste" heat and CO_2. These three zones are numbered and illustrated in Figure 3. Their detailed schedules are described in Table 1.

(1) In green in Figure 3, the Greenhouse Zone (GZ). It is located on the top floor with a large roof window to allow sufficient transmission of light to the plants, with shading in operation when the room temperature reaches 28 °C. This zone acts as a shell for the greenhouse and all input-output exchanges between the BES and the GES-II model occur through this zone. The methodology to include the effect of the plant module modelled in GES-II into BES is explained in Section 4.
(2) The top floor circulation area is called the "Corridor Zone" (CorZ). As pupils fill

[2]The DLI is calculated using the GES-II model equations described in Appendix A.1, as a function of the incoming solar radiation modelled in Energy Plus. The DLI is the sum of the PAR absorbed the plants over a day.

this area regularly (Table 1), the CO_2 levels reach 1400 ppm, and the temperatures are warm. This zone is subject to heating and cooling during term-time.

(3) The south facing classroom on the middle floor, below the GZ, is known as the "Classroom Zone" (ClaZ). The high occupancy rate leads to very high CO_2 levels and temperatures, requiring significant energy use for cooling and ventilation to meet occupant comfort levels.

Table 1. Operational parameters for the three zones of interest in the building model

	Greenhouse Zone (GZ) baseline design	**Corridor Zone (CorZ)**	**Classroom zone (ClaZ)**
Occupancy schedule	weekdays classroom visit at 1pm, 8am and 5pm 2 people maintenance	7-8h 0.1, 8-9h 0.25, 9-16h 0.5, 16-17h 0.25, 17-21h 0.1, else 0 during termtime	7-8h 0.08, 8-9h 0.6, 9-12h 0.8, 12-14h 0.4, 14-16h 0.8, 16-17h 0.4, 17-21h 0.08, else 0 during termtime
Occupancy value	2 morning, 13 classroom visit	0.11 people/m^2	0.55 people/m^2
Ventilation	Varies seasonally and diurnally. Min 4 ACH in winter all day long, max 16.6 ACH in summer during daytime.	7-21h on 0.0012 $m^2/m^2/s$	7-21h on 8 L/person
Heating	6h-21h 16°C , else 13.6°C all year	6h-21h 20°C , else 15°C during termtime, else SP 12°C	6h-21h 21°C, else 15°C during termtime, else SP 12°C
Cooling	6h-20h SP 27°C, else 29.7°C all year	6-21h SP 32°C, else off during termtime	6-21h SP 32°C, else off during termtime
Dehumidification	humidistat 80% all year round	not included	not included
Lighting requirement value	no additional lighting	7-21h on, during termtime 80-120 lux 6 W/m^2	7-21h on, during termtime 300 lux 10 W/m^2
Electric equipment value	not included	7-18h on, rest 0.05 2 W/m^2	7-18h on, rest 0.05 10 W/m^2
Zone mixing	From CorZ and to ClaZ	to GZ	from GZ

2.2.1. Ventilation

In the school ventilation guidelines (DfE 2018), Carbon Dioxide is the main indicator for indoor air quality and ventilation performance: the average CO_2 level during the occupied period should be designed to not exceed 1000 ppm, and the maximum CO_2 level should not surpass 1500 ppm for longer than a 20 minute interval during school hours (i.e. 9-18h). Of particular interest is the classroom ventilation rate. With a peak occupancy rate of 0.55 students/area and zone volume of 756 m^3, 4 ACH is used. This corresponds to approximately 6 L/s/person, which falls between the recommended 3 and 8 L/s/person for classrooms. The ventilation schedule of the GZ is based on Watson et al. (2019), such that summer ventilation is significantly higher than winter ventilation to keep temperatures cool in summer while minimising heating requirements in winter. As such, it is set to 4 ACH in winter months, and increases to 16.6 ACH when temperatures are hottest (in this case in July), during the daytime. Nighttime ventilation is lower than during periods of the day with daylight (e.g ventilation rate in July is 16.6 ACH between 10h and 21h, and 4 ACH otherwise).

2.2.2. Occupants, equipment and lighting

Schedules and values for occupants, equipment and lighting are from DfE (2003) and Dodd, Garbarin, and Caldas (2016). Occupant schedules use the ASHRAE 55 dynamic clothing model to vary clothing level with outdoor temperature and time of day, and vary the metabolic rates, fraction of sensible heat, occupancy levels with the type of activity in the zone. The occupancy schedule in the baseline design of the GZ is set at a classroom visit at 1pm by a group of 13 students on weekdays and two maintenance visits of two people in the morning and evening on weekdays (Table 1). Additional artificial lighting or equipment are not included in the GZ.

2.2.3. Heating and cooling

Heating and cooling loads are specified using the Ideal Loads HVAC system, with temperature setpoints for heating and cooling. DfE (2018) recommends heating setpoints of 18 °C for classrooms, 21 °C for zones with low metabolic activity and 15 °C for circulation areas. As 60% of secondary school buildings have air conditioning, cooling was also included when internal temperatures surpassed 32 °C when the zones are occupied. Heating and cooling for the baseline design of the Greenhouse Zone is also described in Table 1. Typical setpoints for HVAC in greenhouses vary depending if they are passive greenhouses (Léveillé-Guillemette and Monfet 2016), or completely controlled environments (Kozai 2016). For hydroponic lettuce growing, ideal conditions are accepted to be within 18 and 24°C (Brechner, Both, and Staf 1996; Thompson and Langhans 1998). We opted for a passive greenhouse design, and chose heating setpoints of 16 °C during the daytime and 13.7 °C at night. Cooling is activated if internal temperatures surpass 27 °C between 6h and 21h, and 29.7 °C at night. Humidity levels over 80% are known to decrease crop growth due to pathogens (Park and Park 2011), so a permanent humidistat of 80% is also set in the greenhouse.

2.2.4. Zone air mixing

The coupling of the greenhouse and the school building is achieved through the ZoneMixing object in EnergyPlus, which allows one-way flow from a source zone to a receiving zone, creating a convective gain of heat and mass (air, water vapour and CO_2). The air flow rate can have a fixed schedule, or be controlled by the temperature difference between the source and receiving zone. In our case, zone mixing is specified by a flow rate, as a function of the desired mixing rate compared to natural ventilation. As indicated in Table 1, two zone mixing flows are used in this model. The heated and CO_2 rich air in the Corridor Zone is used as an input for the Greenhouse Zone (corZ to GZ). Cool and O_2 rich air from the Greenhouse Zone is introduced into the Classroom Zone (GZ to ClaZ).

2.3. *Building energy demand*

The building energy model is simulated in Energy Plus v8.9, with ideal load specification for the HVAC system. The resulting energy use intensity (EUI) from the BES model alone is between 130 and 140 kWh/m^2, depending on the ventilation and heating settings of the Greenhouse Zone, and without any inter-zone air mixing. Its average EUI of 135 kWh/m^2 is plotted against the school's headcount in Figure 2, which illustrates it is in line with the best practice numbers (Table 5). Energy intensity for electricity demand is 48 kWh/m^2. Energy demand for the HVAC system

varied depending on the Greenhouse Zone parameters set in the BES. If the settings for GZ follow the heating, dehumidification and ventilation requirements described in Table 1, this brought the building annual HVAC demand to 93 kWh/m^2. If the GZ is not included at all, the building HVAC demand is 82.3 kWh/m^2. For a passive greenhouse design, with no plants, low ventilation (1 ACH at most), no heating and cooling, HVAC demand of the building was 81.5 kWh/m^2, suggesting a passive GZ acts as a buffer for the building and its simple presence reduced building energy demand by 1%.

3. Greenhouse Energy Simulator II

To include the dynamic effect of plants in the BES, the greenhouse model GES-II was developed. This time dynamic heat and mass transfer model represents transpiration, photosynthesis, and crop growth in an enclosed environment, and is an adaptation of the Greenhouse Energy Simulator (GES). GES was developed by Ward et al. (2015) and based on the Gembloux Dynamic Model Greenhouse Climate model (Pieters and Deltour 1997), to which the reader is referred to for detailed description of the heat and mass transfer model. The GES model describes the effects of the outdoor climate and greenhouse design on the indoor greenhouse climate with of a set of first order differential equations (ODE) that have been validated in several settings (Vanthoor 2011; Ward et al. 2015), and is written in Matlab (The Mathworks Inc 2016). In the case of GES-II, the effect of the outdoor climate and greenhouse design are input from the BES model, and GES-II calculates the change in internal conditions due to the components unique to a greenhouse - represented by a hydroponic module. This module contains three elements: vegetation (v) which grows on a moist mat (m) which is held in an aluminium tray (t). GES-II models the growth of lettuce as a function of the air temperature, light level and CO_2, as described in Von Caemmerer (2013), and contributes to the heat and mass balance of the zone air (Appendix A).

3.1. *GES-II model outputs*

The environmental conditions of a greenhouse are a result of highly complex 3-D heat and mass exchange between the plants and their surroundings. A key assumption of GES is that a typical greenhouse is regular in layout. Therefore one can simplify the problem to a 1D slice and calculate the time-dependent heat and mass exchange through the different nodes. For our case of a rooftop hydroponic farm, this constitutes the floor (f), light (l), plant module with growing mat (m), tray (t), vegetation (v), internal air (i) and ceiling (c), subject to external fluctuating boundary conditions as illustrated in Figure 4. The green nodes are unique to the GES-II model, and the grey nodes represent input values from the BES model (light, floor and ceiling). The model represents different levels of mat saturation depending on irrigation and simulates the growth of the plants in terms of its changing Leaf Area Index[3] (LAI) as the crops grow. The flows between the nodes are diffuse and direct radiation (R), convection (V), conduction (D), and latent heat (P), and mass flow of carbon dioxide (C).

The main outputs of GES-II at the end of each timestep are thus linked to the unique GES-II components: internal air temperature (T_i), air moisture content (W_i)

[3]Leaf Area Index is defined for flat leaves as the area of leaves per unit area of ground, on one side only of the leaf.

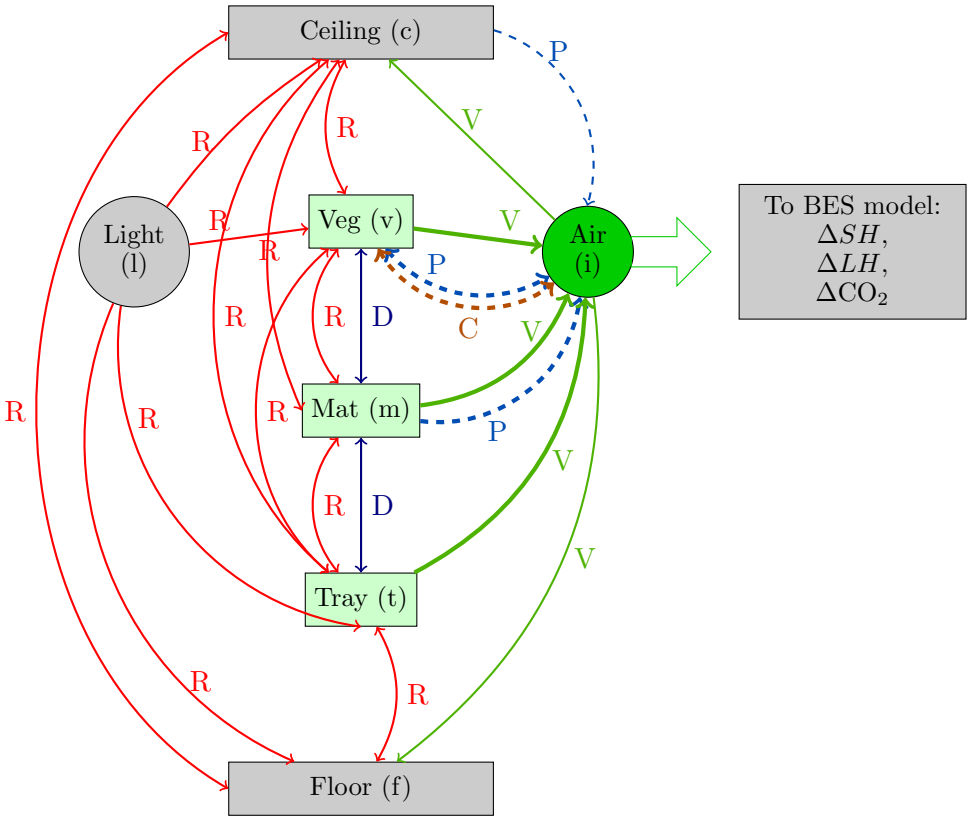

Figure 4. GES-II heat and mass transfer flows between nodes at a given timestep. The grey nodes show the parts of the system which are shared with the BES model, while the green nodes are only modelled in GES-II. Full lines correspond to sensible heat flows, while dotted lines represent mass flows. The flows between the nodes are diffuse and direct radiation (R), convection (V), conduction (D), latent heat (P), and carbon dioxide mass flows (C). The effect of the plant module on the internal air node (i) can be translated into outputs ΔSH, ΔLH, ΔCO_2 which can be transferred to the BES.

and CO_2 concentration (C_i); surface temperature of the growing mat (T_m), tray (T_t) and vegetation (T_v); and accumulated mass of dry matter grown (kg DM/m^2). These can be stored in Matlab for the next timestep, allowing to track the crop growth over the entire simulation period.

Flows to the internal air node (i) are of most interest as it is this node that exchanges information with the Greenhouse Zone of the school building (Figure 4). The effect of the plants in the GZ can be translated into net change in sensible heat (ΔSH), latent heat (ΔLH), and volumetric flow rate of CO_2 (ΔCO_2), from the difference between the environmental conditions input into GES-II from the BES (T_{GZ}, W_{GZ}, C_{GZ}) and the environmental conditions at the end of the timestep in GES-II (T_i, W_i, C_i). These flows are defined in Equations 1 to 3. They can be transferred to EnergyPlus through the so-called External Interface at the end of each timestep.

The sensible heat gain ΔSH in W is calculated in the timestep Δt by:

$$\Delta SH = \frac{T_i - T_{GZ}}{\Delta t} \rho_i c_p V_{GZ}, \qquad \text{(W)} \quad (1)$$

where T_i is the updated temperature output by the GES-II model in Kelvin, and T_{GZ} is the input temperature at the start of the timestep from the BES. The change in sensible heat also depends on the constants V_{GZ} (m^3), volume of the Greenhouse Zone,

and c_p the heat capacity of the air (1003.2 J/kg/K). The density of air ρ_i (kg/m^3) is calculated as a function of the air temperature T_i.

The latent heat gain ΔLH is calculated by:

$$\Delta LH = \frac{W_i - W_{GZ}}{\Delta t} h_{fe} V_{GZ}, \quad \text{(W)} \quad (2)$$

where h_{fe}, the latent heat of vaporisation of the air (2.44×10^6 J/kg), V_{GZ} the zone volume, and W_i is the air moisture content output from the GES-II model in kg/m^3. W_{GZ} is the original Greenhouse Zone (GZ) air moisture content calculated by the BES and sent as input into the GES-II model at the beginning of the time step.

The volumetric change in CO_2 (m^3/s), fed back to EnergyPlus is calculated from the difference of C_i and C_{GZ}, where C_i is the density of carbon dioxide output from the GES-II model in kg/m^3:

$$\Delta \mathrm{CO_2} = \frac{C_i - C_{GZ}}{\Delta T \rho_i} V_{GZ}(10^{-3}), \quad \text{(m}^3\text{/s)} \quad (3)$$

3.2. *Equations of state for internal air*

The three equations of state for the internal air are described in Equations (4) to (6) for temperature (T_i in °C), air moisture content (W_i in kg/m^3) and CO_2 concentration (C_i in kg/m^3). The heat fluxes are referred to as QV (Watts), and the mass fluxes of water vapour and CO_2 as QP (Watts) and MC (kg/m^3/s) respectively. The fluxes have two subscripts indicating the source and destination of the flux.

$$\frac{dT_i}{dt} = \frac{1}{V_{GZ}\rho_i c_i}(QV_{[m\to i]} + QV_{[v\to i]} + QV_{[t\to i]}). \quad (4)$$

QV represents the flow of sensible heat due to convection, for instance $QV_{[m\to i]}$ is the flow from the mat to the internal air, which is function of the temperature difference between the mat and the air.

$$\frac{dW_i}{dt} = \frac{1}{V_{GZ}h_{fe}}(QP_{[m\to i]} + QP_{[v\to i]} + QP_{[t\to i]}). \quad (5)$$

The change in air moisture content of the air depends on the flows of latent heat (QP) due to evaporation from the mat to the internal air ($QP_{[m\to i]}$), and the transpiration from the leaf ($QP_{[v\to i]}$). Both are calculated from the difference between air moisture content of the air and the respective node. The transpiration model from Graamans et al. (2017) is described in the appendix, Equation A11. Evaporation and condensation between air and tray is assumed to be negligible, so $QP_{[t\to i]}$ is set to 0 W.

The temperatures and moisture content of the vegetation, mat, and tray vary in analogous way to the air node i with convection, conduction and radiation flows, as illustrated in Figure 4. The vegetation temperature also varies with transpiration, and evaporation from the mat is related to its saturation level.

The change in CO_2 concentration C_i is attributed to the difference between carbon assimilation through photosynthesis and maintenance respiration of the plants (Equa-

tion 6). The rate of change of CO_2 is calculated as a function of mass flow rate of carbohydrates MC in the plant system (kg/m^3/s), between the buffer MC_{buf}, leaf MC_{leaf} and stem MC_{stem} and the internal air C_i (all in kg/m^3). The crop growth model is based on Farquhar, von Caemmerer, and Berry (1980); Von Caemmerer (2013); Bonan (2015), where the carbon assimilation rate varies with three limiting states: atmospheric CO_2 and the enzyme Rubisco which catalyses CO_2 fixation (Equation (A23)), light and electron transport (Equation (A24)), and starch accumulation (Equation (A26)). Detailed model equations are described in the appendix.

$$\frac{dC_i}{dt} = \frac{M_{CO_2} A_p}{M_{CH_2O} V}(MC_{[buf \to i]} + MC_{[leaf \to i]} + MC_{[stem \to i]} - MC_{[i \to buf]}), \qquad (6)$$

where M_{CO_2} and M_{CH_2O} are the molar mass of CO_2 and carbohydrates respectively.

The amount of carbon sequestered by the plant in the organs C_{leaf} and C_{stem} indicates the level of crop growth, and thus the LAI. When C_{leaf} reaches its threshold harvest level, the crop is harvested, reducing the crop volume in the greenhouse. LAI in turn impacts the transpiration rates and the solar radiation interception. The mass of carbohydrates is known as the dry matter (DM), which is directly proportional to the harvested fresh weight (FW) of the plant (Equation A34).

As previously mentioned, three environmental factors limit the rate of photosynthesis: light, temperature and CO_2 (Blackman 1905). Photosynthesis and transpiration have been shown to be almost proportional to solar radiation (Tei, Scaife, and Aikman 1996). However, a daily light integral of maximum 18 hours is essential for crops to maintain their circadian rhythm and maintenance respiration phase (Davis 2015). Photosynthesis is also inhibited by temperatures which are too low or too high, and the optimal temperature of lettuce is set between 18 and 24 °C (Vanthoor 2011). Increased CO_2 concentration also increases the rate of gas exchange with the plant (Bonan 2015), which motivates CO_2 enrichment of greenhouses. The environmental factors tend to be limiting at different times of day, so for example CO_2 enrichment would be unnecessary if there is no light (Ferentinos, Albright, and Ramani 2000). The water content and size of plants also increase with transpiration, a function of vapour pressure deficit and solar radiation (Tibbitts and Bottenberg 1976). Relative humidity must therefore be kept high but under 80% to avoid mould from condensation on the leaves (Park and Park 2011). This is controlled by a dehumidifier in the BES model.

4. Co-simulation methodology

This section presents the methodology and considerations to co-simulate the two models described above, and the resulting effect on the heat and mass balance in the Greenhouse Zone. The co-simulation process is illustrated in Figure 5. Data is exchanged between the Greenhouse Zone (GZ) of the BES model and GES-II through the Building Controls Virtual Test Bed (BCVTB) software environment. By using the MLE+ tool developed by Bernal et al. (2014), the BCVTB can be configured through Matlab, with the Ptolemy II external interface in EnergyPlus. The BES model calculates the indoor environmental conditions of the GZ and sends them as inputs to GES-II. In turn, the change in heat and mass calculated by GES-II is input into the Greenhouse Zone (GZ) of the BES model. The data is exchanged though an XML variable configuration file, and is detailed in the following subsection. The advantage

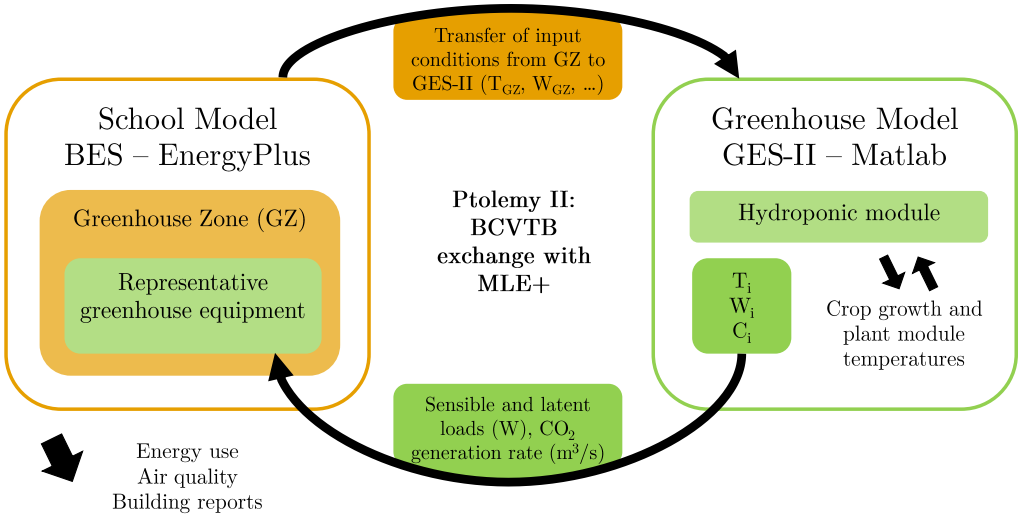

Figure 5. Co-simulation setup between the Greenhouse Zone (GZ) of the BES model in EnergyPlus and GES-II in Matlab. The curved arrows symbolise the exchanged data between the two models at each timestep. The straight black arrows indicate the stored data in each model.

of this methodology is that unique outputs to each model can be stored while the data is exchanged (straight black arrows in Figure 5). As such, the BES model can produce building reports, estimate energy use of other zones, while the GES-II models can keep track of crop growth and harvests, and plant module temperatures.

The timestep chosen for the data exchange of the co-simulation is 15 minutes, as it is the most stable timestep which works for both models. On the one hand, it is the largest recommended timestep in the BES model as EnergyPlus uses a Predictor-Corrector approach, where the heat and mass balance is predicted at the beginning of the timestep to estimate supply air of the HVAC system, and corrected at the end of the timestep with the resulting HVAC inputs. On the other hand, the ODE solver of GES-II is more stable at larger timesteps as it requires "warm-up" iterations to initiate the solver after the data exchange. This short timestep also keeps the assumption stable that the boundary conditions transferred from BES to GES-II are constant over the timestep.

4.1. *Variable exchange*

Recall that the Greenhouse Zone (GZ) of the EnergyPlus model acts as a shell for the greenhouse and all input-output exchanges between the BES and the GES-II model occur through this zone. The exchanged variables are listed in Table 2. All variables are configured in the XML exchange file. Variables from BES to GES-II are sourced from the EnergyPlus Output:Variable object. In contrast, the three returned variables are sent to the ExternalInterface:Schedule object, where they are called by three representative equipment objects linked to the GZ.

Table 2. Parameters exchanged between the Greenhouse Zone (GZ) of BES and GES-II

Exchange direction	**Parameter**	**Unit**	**EnergyPlus Object**
From BES to GES-II	GZ Air Temperature	°C	Output Variable
	GZ Relative Humidity	%	Output Variable
	GZ CO_2	ppm	Output Variable
	GZ Floor Temperature	°C	Output Variable
	GZ Ceiling Temperature	°C	Output Variable
	GZ Solar radiation transmitted through window (diffuse and direct)	W	Output Variable
	Site Air temperature	°C	Output Variable
	Site Wind speed	m/s	Output Variable
	Site Air pressure	Pa	Output Variable
From GES-II to BES	Plant module sensible heat gain ΔSH	W	External Interface Schedule, Other Equipment
	Plant module latent heat gain ΔLH	W	External Interface Schedule, Other Equipment
	Plant module volumetric change in CO_2	m^3/s	External Interface Schedule, Zone Contaminant Source or Sink

4.1.1. Variables from GES-II to BES

The effect of the plants on the environmental conditions in the Greenhouse Zone is calculated by the GES-II model and transferred back to EnergyPlus through the External Interface Schedule component at the end of each timestep. The change in temperature is represented using EnergyPlus's Other Equipment component with a Fraction Radiant of 1. The change in relative humidity (RH) is represented with a second EnergyPlus Other Equipment component with a Fraction Latent of 1. The change in CO_2 concentration is characterised using the Zone Contaminant Source or Sink component, with a volumetric generation rate. In this case, the external interface schedule must be a value between 0 and 1 (Equation 3).

4.1.2. Variables from BES to GES-II

The GES-II inputs from BES correspond to the internal environmental conditions in the GZ and the site environmental conditions. In addition, the surface conditions of the floor and ceiling are transferred to GES-II, as indicated with the grey nodes in Figure 4.

As the surface temperatures are assumed constant over each timestep in GES-II, they are subject to additional consideration. They are modelled in BES by the sum of long and short wave radiation, conduction and convection (Equation 7).

$$\underbrace{q''_{LWX} + q''_{SW} + q''_{LWS} + q''_{sol}}_{\text{Radiation}} + \underbrace{q''_{ki} + q''_{conv} + q''_{add}}_{\text{Conduction/Convection}} = 0. \tag{7}$$

where q''_{LWX} is the longwave radiant exchange (LW) from internal surfaces, q''_{SW} is the shortwave radiation from any internal lights, q''_{LWS} is the LW radiation from internal equipment, q''_{sol} is the solar radiation, q''_{ki} is the conduction through the wall, q''_{conv} is the convective heat flux, and q''_{add} is the additional sensible heat transferred back from the GES-II model to the BES Greenhouse Zone (GZ).

In reality, the planted area would affect the surface temperature of the GZ floor by blocking radiation. Figure 6 illustrates this by showing the hourly difference in floor temperatures of the GZ with and without a large rooftop window across the four

seasons, modelled without the greenhouse. At midday in Spring and Summer months, the floor temperature tends to be 20 °C warmer on average with a large rooftop window than without a window (referred to as base floor temperature T_{f0}). This temperature reduction of the GZ floor needs to be accounted, as it is sent as input to the GES-II model.

Two methods were considered to include this temperature reduction: the use of an internal mass object in the GZ of the BES to represent the thermal inertia of the plants, or the application of a linear reduction proportional to the planted area in the GES-II model. To avoid double counting thermal inertia of plants in both models, the floor temperature, T_f^{GES-II}, passed to the Greenhouse Model are subject a linear relationship with the planted area, described in Equation 8.

$$T_f^{GES-II} = T_{f0} + (1 - A_p)\ (T_f^{GZ} - T_{f0}), \qquad (°C) \quad (8)$$

where T_{f0} is the fixed floor temperature of the Greenhouse Zone (GZ) simulated without the rooftop window for that timestep, T_f^{GZ} is the floor temperature output from BES for that timestep, A_p is the proportion of planted area respective to the surface area of the zone (-). While this method allows to have a more realistic floor temperature in the GES-II model, its main limitation is that it does not modify the floor temperature in the BES model. The effect of this assumption on the rest of the building is limited by assuming the surfaces are adiabatic in EnergyPlus (no surface heat transfer between zones).

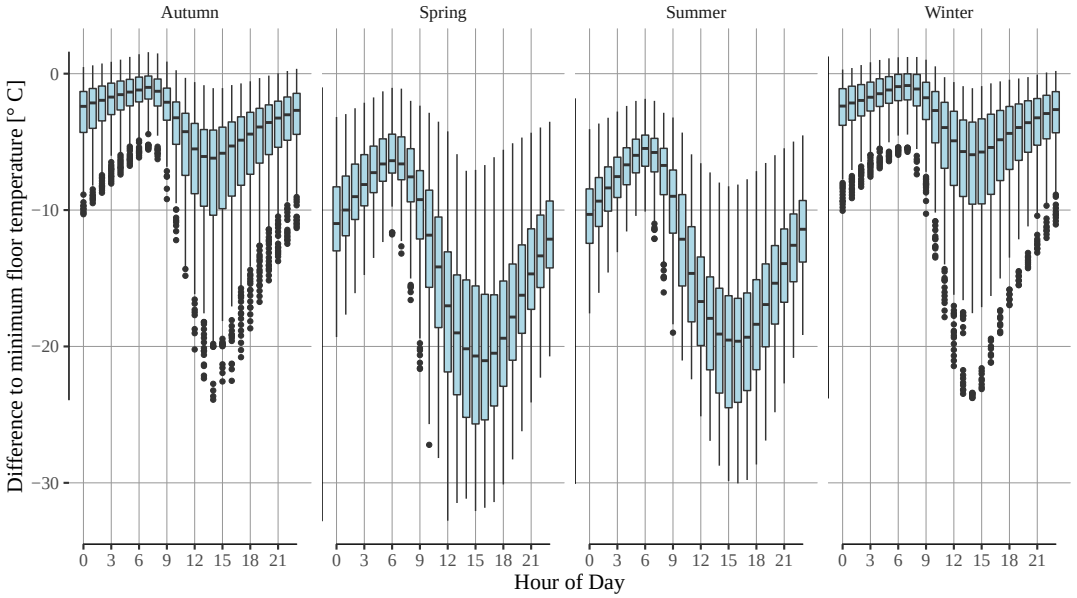

Figure 6. The difference of floor temperature with and without a large rooftop window (area of $0.85A_{GZ}$), separated by seasons.

4.2. *The energy balance in the greenhouse zone*

Both BES and GES-II are heat and mass transfer models that calculate the change of the internal air in the Greenhouse Zone (GZ) for the same three state variables:

temperature, air moisture content, and CO_2 concentration.

In the BES model, the Greenhouse Zone (GZ) is subject to scheduled loads and interacts with its surrounding environments. The net change in temperature T_{GZ} in the Greenhouse Zone (GZ) is calculated through the sum of the following flows (Equation (9)):

$$V_{GZ}\,\rho_{GZ} c_p \frac{dT_{GZ}}{dt} = QV_{loads} + q_{[CorZ \to GZ]} \rho_{GZ} c_p (T_{CorZ} - T_{GZ}) + QV_{surf} + QV_{inf} + QV_{HVAC}. \tag{9}$$

The sum of convective internal loads QV_{loads} represents the sensible heat flows from any scheduled loads from which convective heat is transferred, such as people, lighting or electrical equipment included in GZ. This is also where the "Greenhouse Sensible Heat effect", defined as ΔSH in Equation 1, is included. Air is transferred from the Corridor Zone (CorZ) to the GZ through an exhaust fan at rate $q_{[CorZ \to GZ]}$, and contributes to the heat and mass balance of the GZ, as a function of the two zones' temperature difference. Air temperature also changes due to surface convection QV_{surf}, infiltration from the outside air QV_{inf}, and the heating and cooling load QV_{HVAC} derived from the heating setpoint and HVAC system parameters. These flows are calculated as standard in EnergyPlus, as specified in Section 2.

The change in air moisture content W_{GZ} (kg/m^3) is the analogous mass balance to the heat balance in Equation 9, with latent heat flows QP. The "Greenhouse Latent Heat effect" is included in QP_{loads}. The surface convection QP_{surf} depends on the evaporation enthalpy of the materials. The infiltration load QP_{inf}, and HVAC system load QP_{HVAC} depend on the humidity and temperature of the GZ:

$$V_{GZ}\,h_{fe} \frac{dW_{GZ}}{dt} = QP_{loads} + q_{[CorZ \to GZ]} \rho_{GZ} h_{fe} (W_{CorZ} - W_{GZ}) + QP_{surf} + QP_{inf} + QP_{HVAC}. \tag{10}$$

The mass balance of carbon dioxide (kg/m^3) is calculated in an analogous way to air moisture (Equation 10), except that it does not include the terms for surface convection and the HVAC system.

4.3. *Sensitivity analysis of the co-simulation model*

This co-simulation methodology can be used as a decision-making tool to optimise the design of the coupled configuration of a greenhouse in a building. A simulation-based design problem can be solved more efficiently if the main influential model parameters with respect to a quantity of interest can be identified. Sensitivity analysis (SA) is the ideal mechanism to do so, and has been applied extensively in BES modelling (Tian 2013; Nguyen and Reiter 2015; Menberg, Heo, and Choudhary 2016). The simulation results from the SA runs are then analysed as a parametric study to identify different optimal building-greenhouse configurations.

4.3.1. Model outcomes of interest

Four model outcomes are chosen to represent four objectives of this BIA case study: reduce energy demand for the coupled configuration, achieve high crop yields, find the most optimal way to grow crops efficiently, and maintain good air quality in the classroom.

(1) **Energy use intensity (EUI)** for the conditioning of the greenhouse and classroom zones kWh/m^2/year. The total EUI (EUI_{tot}) is calculated from the sum of energy demand for heating and cooling the Greenhouse Zone (E_{GZ}) and the Classroom Zone below it (E_{ClaZ}), and the energy use for the air transfer from Corridor Zone to GZ, and from the GZ to the Classroom Zone, each with flow rates $q_{[CorZ \to GZ]}$ and $q_{GZ \to ClaZ}$ respectively. These two zones have been selected rather than the total building energy demand to better distinguish the relative effect of the design parameters on the GZ energy use and the potential benefit on the energy demand of its linked Classroom Zone.

$$EUI_{tot} = \frac{E_{GZ} + E_{ClaZ} + \Delta P(q_{[CorZ \to GZ]} + q_{[GZ \to ClaZ]})}{A_{GZ} + A_{ClaZ}} \tag{11}$$

where ΔP is the pressure difference of the zone mixing exhaust fan, calculated with a Specific Fan Power (SFP) of 1 kPa (Railio and Mäkinen 2007; Mysen and Schild 2009) and a total fan efficiency of 0.7.

(2) **Total crop growth**: Crop growth is computed as the total harvested dry matter (DM) of lettuce after a year per unit of area of the GZ. The total harvested fresh weight (FW) of lettuce produced in the GZ over a year (t/year) is .

(3) **Crop growth efficiency**: derived from the total harvested weight and the the sum of energy use of the ClaZ and GZ in g/kWh.

(4) **Air quality in the classroom**: although recovering the heat from different zones will reduce energy use in winter, this variable tracks if there are any implications on the air quality in the Classroom Zone during occupied hours. Lower CO_2 values when there is air transfer from the GZ could quantify the potential reduction in CO_2 from plant photosynthesis. This is measured by the number of days the CO_2 was over 1500 ppm in the classroom for over an hour (minimum requirement in DfE (2014), and the average CO_2 on days the classroom was occupied between 8am and 6pm. No further occupant comfort models are considered, as it is assumed that the dehumidification in the GZ, and the HVAC in the ClaZ are likely to ensure comfortable internal temperatures and humidity according to DfE (2018), and we particularly want to investigate the effect of the planted area on CO_2 levels.

4.3.2. SA input parameters

Seven input parameters are selected as important drivers of energy demand and indoor environmental conditions. The input parameters could be varied in the EnergyPlus and Matlab models by developing a Python module, based on the `eppy` package (Santosh 2019). This allowed to modify inputs in both GES-II and BES. The upper and lower bounds of each input parameter, and the "baseline" scenario value are presented in Table 3.

(1) **Cooling setpoint of the greenhouse**: to analyse the effect of over-heating due to the large roof window, a cooling setpoint is varied uniformly between 26 and 29 °C. This is expected to affect crop yields as well as overall energy use intensity for the two zones of interest.

(2) **Heating setpoint of the greenhouse**: varied uniformly between 15 (rare heating) and 18 °C (typical greenhouse heating setpoint), to evaluate the effect of stable temperatures on crop growth, compare the efficiency of recovering heat from the building compared with heating the GZ to optimal conditions.

(3) **Planted area**: affecting crop yield as well as humidity levels, the planted area is varied uniformly between 0.1% and 99.9% of the floor area.
(4) **Air transfer from the CorZ to GZ**: the ventilation rate in the GZ is scheduled to vary seasonally and diurnally as per greenhouse ventilation guidelines (Watson et al. 2019). The proportion of heated and CO_2 rich air coming in from the corridor zone is varied between 0 to 1.
(5) **Air transfer from the GZ to the ClaZ**: the ventilation rate in the ClaZ is set to meet school guidelines for classrooms (Section 2). The proportion of ventilation air coming from the GZ through air mixing is also varied from 0 to 1. This variable is expected to have an effect on humidity levels in the classroom, occupant comfort, and energy use. The effect of increased RH in the classroom is expected to be quantified through increased energy demand for dehumidification, counteracting the potential decreased energy demand for heating.
(6) **Rooftop window shading**: the solar transmittance of the shade was varied uniformly between 0.01 and 0.98. The shading is only scheduled if the greenhouse zone temperature surpassed 28 °C.
(7) **Greenhouse window size**: the large rooftop window in the greenhouse allows natural sunlight to be harvested for the growth of plants, but also generates large solar gains, and decreases the U-value of the roof in winter. The window size is varied from 50% to 90% of the roof area.

It is important to note that the choice of these seven parameters is driven by their likely influence on the coupled BES and GES-II model outputs, rather than an individual quantity of interest. For example, air quality of the classroom is influenced by occupancy levels and infiltration in addition to ventilation rate. However, these are not included in the sensitivity analysis as they will not have any impact on the co-simulation.

4.3.3. SA methods

As standard in SA, we consider the outcome of building energy simulation as mathematical function $\mathbf{Y}(\mathbf{x})$ with $\mathbf{Y}$ a matrix of the three model outputs of interest, and $\mathbf{X}$ as a $N \times k$ matrix, with N samples of $k = 7$ input parameters, defined in the parameter space by lower and upper bounds for each parameters. To ensure consistency, we compare the outcomes from two commonly applied SA methods: the Standard Regression Coefficient method and the Morris' parametric method. For a detailed review of the methodology, see Menberg, Heo, and Choudhary (2016).

Estimating the Standard Regression Coefficients (SRC) gives an indication of the extent to which each variable influences the outcome, but requires a large number of simulations. To limit this, we use latin hypercube sampling to provide better coverage of the parameter space than random Monte Carlo samples, as it initially partitions the parameter space into equally probable areas, from which random samples are drawn within these multidimensional areas. Given our seven input parameters, 50 such samples were considered sufficient, leading to a total of $N = 350$ simulations. The regression coefficients are calculated for each model outcome by approximating a multivariate linear model to fit the model response. The estimated regression coefficients can be compared by standardising them using the variance of the model response and the variance of the corresponding input parameter. The absolute value of the SRC represents the importance of each parameter on a scale of 0 to 1, while its sign indicates whether it positively or negatively impacts the model outcome.

The Morris method uses parameter screening in combination with a factorial sampling strategy to reduce the number of simulations to perform in order to have a qualitative ranking of parameter importance. It is designed to inform more on which parameters are negligible rather than which are most important. The parameter screening method involves choosing a number of trajectories r for each input parameter. For our study of 7 input parameters, we chose $r = 12$ trajectories, according to Menberg, Heo, and Choudhary (2016). A trajectory is defined for each parameter as a sequence of $k+1$ points, starting from a random point selected from a regular grid with for unit length the hypercube H^k. Within a trajectory, each parameter changes by the increment Δ_i of the trajectory. This is repeated for each parameter, for a total of $N = 96$ simulations. The elementary effect is then defined as the magnitude of variation in the model output due to a the variation of one parameter X. The effect of the parameter on the model can be evaluated through absolute mean of the EE within a trajectory μ^*. This statistic is in the same unit as the model outcome.

5. Results

5.1. *Co-simulation outputs*

Whilst we do not have data to perform a form of model validation, it is possible to check that the outputs from the co-simulation are within reasonable expectations. To investigate the effect of including the GES-II into the Greenhouse Zone in BES, we test the model with two scenarios: (a) "No plants", where the planted area represents 1% of the floor area, and (b) "Full plants" where 98% of the floor area is covered with plants. The "Full plants" planted area A_p is not aimed to represent a real farm but is assumed to test the influence of a large volume of plants. Such large planted areas can however be achieved if vertical hydroponic systems are used, although they may require additional artificial lighting (e.g. 103% of floor area in Jans-Singh et al. (2020)).

Results from the different simulations are presented in Figure 7 for a 24 hour period in August to show the effect of updating the BES model with the inputs received from the GES-II model. Internal conditions are represented by coloured lines with "No plants" scenario in blue, and "Full plants" in yellow. A further distinction is made between dotted and solid lines. The dotted lines for both scenarios are the outputs from the GES-II model and the solid lines represent the outputs from EnergyPlus after they are updated with the inputs received from the GES-II model. Under the "No plants scenario" one would expect the GES-II and BES model outputs to be almost similar. Indeed, comparing the blue solid and dotted lines, we see that the outputs from the two models are consistent.

For the scenario when 98% of floor area is covered with plants, we expect the GES-II model outputs to have an influence on the updated BES output. Comparing the yellow dotted line (the final updated BES output) against the solid lines, it can be noted that the presence of plants causes decrease in CO_2, increase in humidity, and decrease in temperature.

A comparison of the blue and yellow dotted lines serves to show the large influence of plants on the GES-II ouputs. Indeed, it shows the significant change in all three parameters due to the presence of plants. The net change in the BES output, as represented by the solid yellow line, is not so large. This is because the heat and mass fluxes in EnergyPlus model includes other sources/sinks: for example, infiltration and

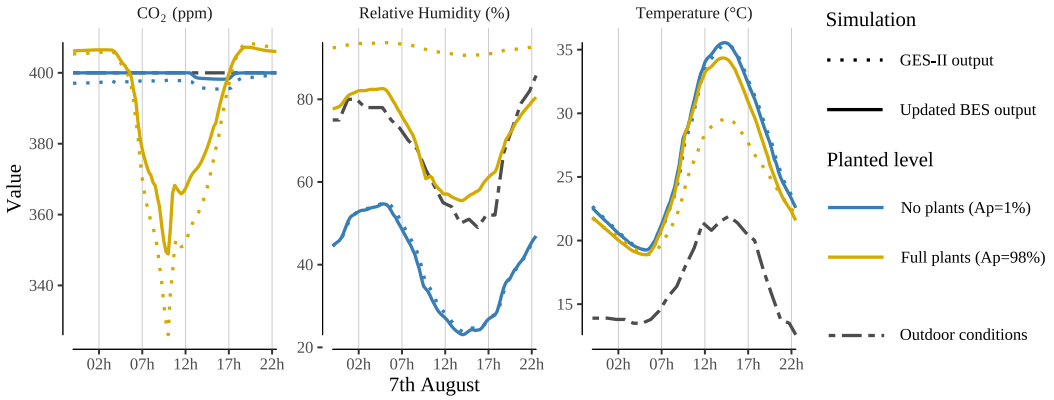

Figure 7. Effect of the plant module on temperature, relative humidity and CO_2 concentration for one day in August. The line type refers to the simulation level: dotted - GES-II output at the end of the timestep, solid - updated BES output after input from GES-II. The planted level indicates the outputs for the two scenarios: "No plants" ($A_p = 1\%$ of floor area) and "Full plants" ($A_p = 98\%$ of floor area).

ventilation with outside air (Equations 9 and 10).

The relative effect of the sensible and latent heat flows calculated by the GES-II can be observed in Figure 8 for three typical days in August when there are "No plants" (left) and "Full plants" (right). No heating, cooling, dehumidification, occupant or equipment schedules were included in the BES to compare the effect of the exchanges from GES-II more accurately. The latent heat transfer increases (with some lag) when there is radiative heat gain through the window, pointing to the start of the daily transpiration process. Latent ventilation loss is prominent at the same time, showing that ventilation regulates the relative humidity, which would have otherwise been very high. Sensible heat loss, on the other hand, does not have such a pronounced effect, due to the thermal storage of the plants counteracting the decrease in temperature from evapo-transpiration. These flows explain the difference between the relative humidity and temperature output from GES-II and the updated BES output in Figure 7.

5.2. *Sensitivity analysis*

The model outcomes for the co-simulation model when using the upper bound and lower bound values of model input parameters are shown in Table 3. Each parameter was set in turn to the upper and lower bound defined in the range, while fixing all the others to the specified mean value. The mean and standard deviation across all the model outcomes is presented in the first row. These values are very close the baseline (modelled with the mean of the input values and listed in the bottom row of table 3) which shows that the mean of each output is in accordance with literature. Average energy demand for both zones is 158 ± 20 kWh/m^2/year, in accordance with school building energy use (Table 5). Average yields are of 3.3 kgDM/m^2/year, in line with Vanthoor (2011) where tomato crop yields over 6 to 9 months were from 0.9 kgDM/m^2/year to 3.3 kgDM/m^2/year, depending on the greenhouse design. The higher yields here reflect the multiple crop harvests possible with a lettuce model (no fruit development). The mean CO_2 during occupied periods in the classroom is 882 ppm, suiting the design requirement of a mean less than 1000 ppm, which should be achieved if staff open the windows according to the design ventilation requirements (Coley and Beisteiner 2002).

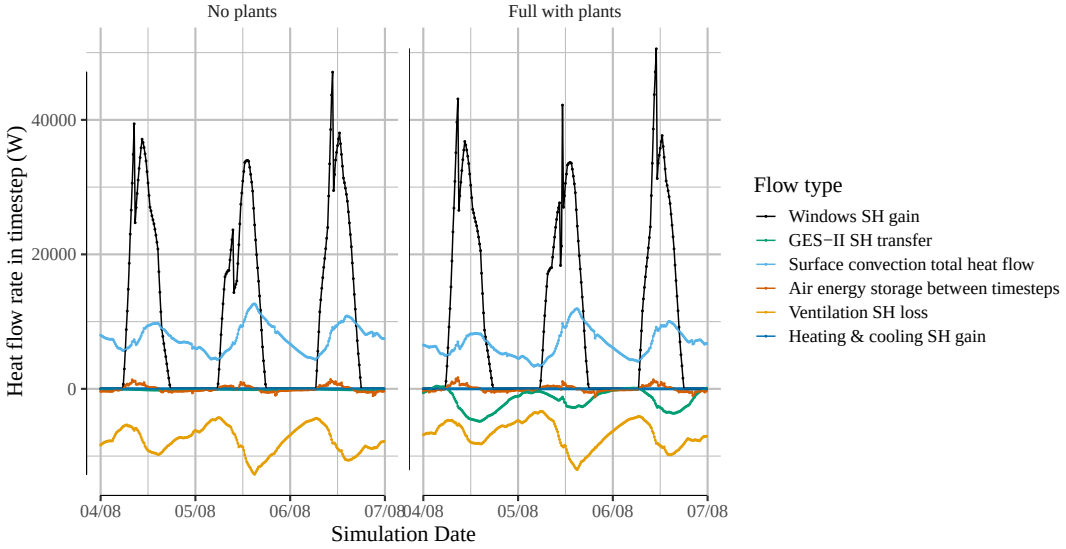

(a) with sensible heat flows from GES-II to the BES GZ

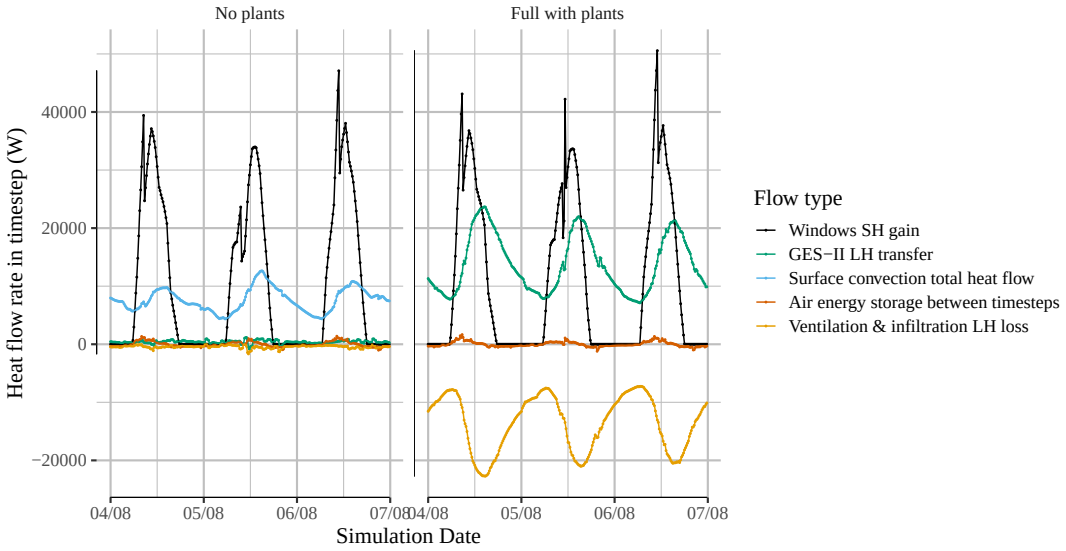

(b) with latent heat flows from GES-II to the BES GZ

Figure 8. Sensible and latent air heat balance flows in the greenhouse zone over three days in August, without plants (left), and full of plants ($A_p = 98\% A_{GZ}$). The flows are: windows SH gain (black), GES-II latent and sensible heat transfers (green), total surface convection rate (light blue), heat stored in the zone air between timesteps (red), ventilation sensible and latent heat loss (orange), heating and cooling SH gain (dark blue).

Compared with the baseline, the energy use intensity increases by 30% when the heating setpoint temperature in the greenhouse is raised from 15 to 18 °C, while only increasing yield by 3%. In contrast, the ventilation rate in the greenhouse, shading, and planted area have little effect on EUI (Table 3). We thus expect greenhouse heating and cooling setpoints and the ratio of air mixing from the corridor to the greenhouse to be the most influential parameters for EUI. Occupant comfort levels will mostly be determined by the ventilation rate in the classroom and the proportion of incoming air from the Greenhouse Zone. We expect crop growth to be influenced by proportion

Table 3. Upper and lower bounds of the SA input parameters, and their result on the four outcomes of interest. EUI: Energy Use Intensity of the GZ and ClaZ. CG: Annual crop growth. CGE: Crop growth efficiency. AQ: Air quality in the ClaZ. UB and LB: results from using upper bound and lower bound of input parameter.

Input variables				**Model outcomes**							
				EUI_{tot} kWh/m^2/year		**CG** tDM/m^2/year		**CGE** gFW/kWh/year		**AQ** ppm	
Location	**Variable name**	**Mean**	**Range**	**LB**	**UB**	**LB**	**UB**	**LB**	**UB**	**LB**	**UB**
	Mean ± std			158 ± 23		3.3 ± 0.3		45.5 ± 13.7		875 ± 61	
Greenhouse Zone (GZ)	(1) Cooling setpoint (°C)	27	[26, 29]	167	120	3.4	3	55.3	75.7	905	906
Greenhouse Zone (GZ)	(2) Heating setpoint (°C)	16	[15,18]	145	188	3.3	3.4	47.7	65.6	905	906
Greenhouse Zone (GZ)	(3) Planted area (%)	0.5	[0.01, 0.99]	135	171	3.6	3.1	1.5	96.9	907	904
Corridor Zone to Greenhouse Zone	(4) Ratio of air mixing (%)	0.5	[0.01, 0.99]	194	145	3.1	3.6	40.5	72.6	812	1003
Greenhouse Zone to Classroom Zone	(5) Ratio of air mixing (%)	0.5	[0.01, 0.99]	177	153	3.4	3.4	57.7	60.2	786	1052
Greenhouse Zone (GZ)	(6) Shading transmission (%)	0.5	[0.01, 0.99]	158	157	3.3	3.4	57.5	59.7	905	906
Greenhouse Zone (GZ)	(7) Size of rooftop window (%)	0.7	[0.5, 0.9]	133	182	2.7	4	58.3	58.4	906	905
Baseline	*With mean conditions*			157		3.4		59.7		905	

of incoming air from the corridor, rooftop window size, shading, and planted area.

The sensitivity analysis shows alignment between the rankings of input parameters from the Morris method and the SRC method, validating our confidence in the results. This is displayed in Figure 9, where the absolute value of the SRC is plotted against the absolute mean of the elementary effect μ^*. Future analysis can thus confidently be performed with either method. The coefficient of determination for the regression of each model outcome with the SRC method was 0.95, showing that the regression model produced with the input parameters explains 95% of the variance observed in the corresponding output. While the SRC gives information on the relative importance of the input parameters, the Morris method allows to distinguish influential from "unimportant" factors (Campolongo, Cariboni, and Saltelli 2007). Both methods show the same ranking of input parameters for all outcomes, but crop yield represented in Figure 9C stands out. The large μ^* values (54 kgFW/m^2/year to 121 kgFW/m^2/year) including for the lowest ranked parameters "Heating GZ" and air mixing "GZ-ClaZ", which have a SRC< 0.2, suggest that none of the input parameters are negligible for crop growth.

All input parameters apart from shading and mixing of air from GZ to ClaZ had a significant influence on the energy demand in the GZ (Figure 9A). The most impactful is air mixing from the corridor to the greenhouse, highlighting the large potential in heat recovery from the building. Changing the cooling setpoint by 3 °C has a similar effect as changing the heating setpoint by the same amount on energy use in the GZ, but cooling influenced the crop growth outcome more. Finally, the size of the rooftop window and planted area also have a non-negligible effect on energy demand in the greenhouse over a year.

As air mixing from the GZ to the ClaZ is the only parameter directly affecting the classroom energy demand in this SA, it is unsurprising that it outweighs the significance of the other input parameters in Figure 9B. The only other parameter with influence on this energy demand is air mixing from CorZ-GZ, suggesting that coupling air transfer to and from the GZ can yield energy saving benefits. Greater

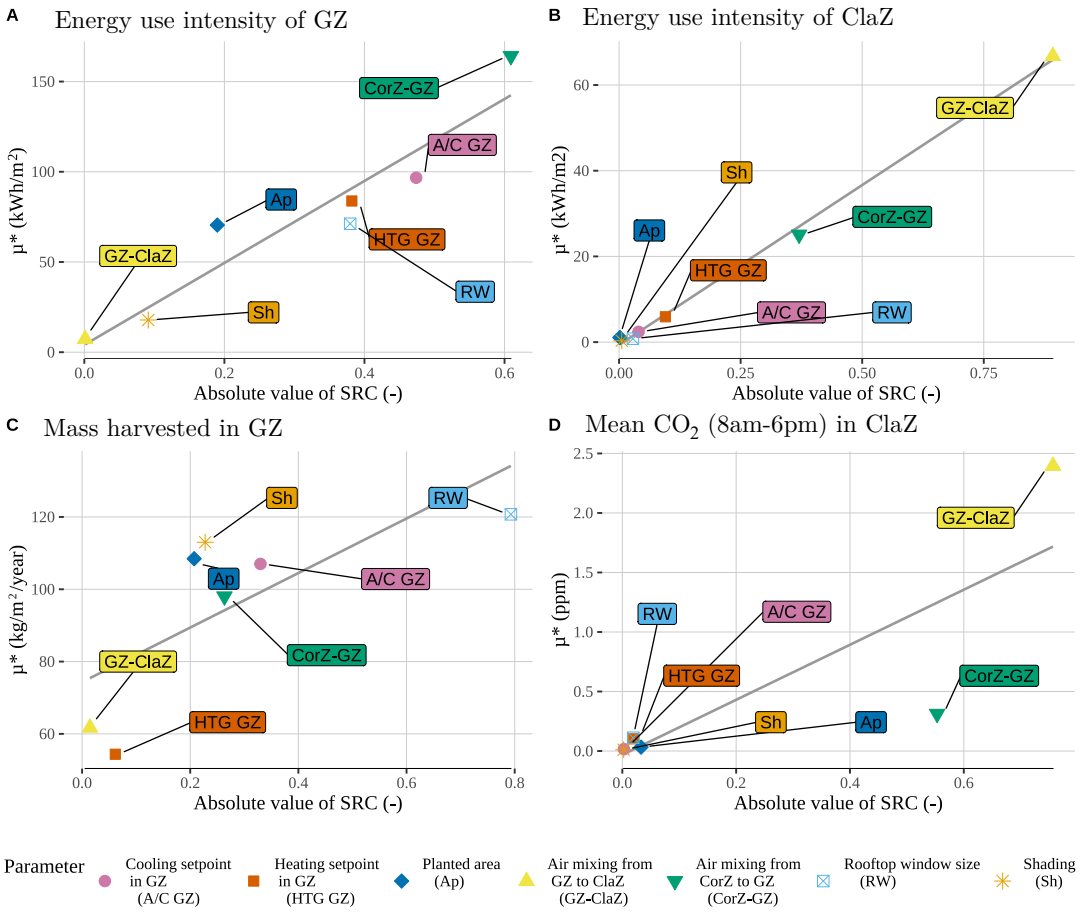

Figure 9. Comparing SRC coefficients (-) and Morris method elementary effects ($\mu*$) for four annual model outcomes: (A) energy use intensity of the greenhouse (kWh/m^2/year), (B) energy use intensity of the ClaZ (kWh/m^2/year), (C) total Dry Matter grown over 1 year per unit of cultivated area (kgDM/m^2/year), and (D) mean CO_2 in ClaZ on occupied days between 8pm and 6am (ppm).

air mixing does however increase the CO_2 concentration in the ClaZ (Figure 9D). Thus, CO_2 levels ought to be monitored to not exceed guideline values, as the "air purifying" effect of the plants in the GZ is not notable. Combining this study with more fine grained controlled ventilation modelling would allow increased sensitivity to the energy saving potential of recovering air from the GZ.

As SRC coefficients inform on the direction of influence of the parameters, the SRCs were further analysed by season. The seasons were defined by splitting the model responses such that Winter is from January to March, Spring is from April to June, Summer is from July to September, and Autumn is from October to December. The SRCs for air quality showed little seasonal difference over the year compared with Figure 9. However, the seasonal breakdown for these three SA outcomes: (A) crop growth efficiency, (B) energy demand of the GZ and ClaZ (EUI_{tot}), and (C) total crop yields, reveal how different co-design strategies can be implemented throughout the year. For instance, while looking at the whole year response suggests that increasing the heating setpoint would have only a limited impact on crop yield, the SRC coefficient in winter in Figure 10C shows that it does have an effect on increasing the crop yield in winter months. A design strategy to encourage early crop growth in the year would

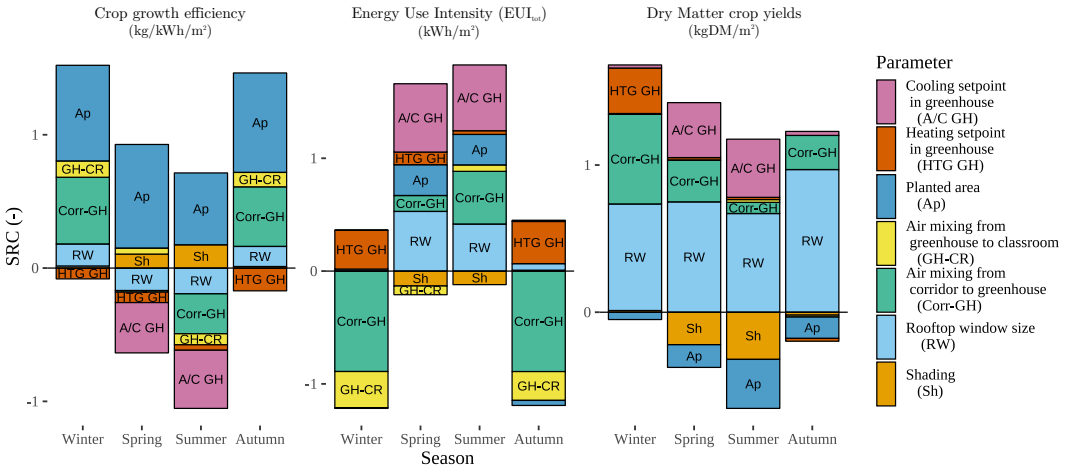

Figure 10. SRC calculated for four seasonal subsets for three model outcomes: (A) crop growth efficiency (g fresh weight (FW)/kWh), (B) total EUI of ClaZ and GZ, and (C) accumulated Dry Matter over a year per unit of cultivated area.

be to have additional heaters in winter, which would not be necessary throughout the rest of the year, simply causing a high energy cost. In summer months, shading is the only input parameter reducing energy demand of the coupled configuration, and the rooftop window size is less important as it also causes overheating. Crop growth in the greenhouse also benefits from air mixing from the Corridor Zone mostly in Winter and Spring, but is not necessary in Summer. The larger positive SRCs of the CorZ-GZ zone mixing compared with the heating setpoints on crop yields (Figure 10C) highlight the benefits of CO_2 enrichment to the greenhouse with air from the circulation area.

Larger planted areas negatively influence crop growth in Summer, presumably due to their faster growth rate and thus larger LAI which could inhibit growth on lower leaves, and increase humidity. Humidity is accounted as having a high energy cost due to the dehumidification setpoint in the GZ of 80%. If the main concern is reducing energy use intensity rather than creating the optimal crop growth environment, cooling should be avoided in summer, and a smaller rooftop window could be considered. Without having an impact on crop yields, heat exchange from the greenhouse zone to the classroom zone reduces the overall energy use and should be considered in Winter and Autumn months. The three different SA outcomes suggest further conflicting advice based on the objective of the designer. Large planted areas cause lower crop yield per unit area, and higher energy demand per unit area, but to different extents. On the other hand, it is shown in Figure 10A that planted areas should be maximised for high crop growing efficiency.

5.3. *Parametric analysis*

The simulation runs for the SA are used for a parametric study to evaluate different design configurations in relation to the model outcomes. Table 4 gathers the results of the "best case scenarios" when optimising for low energy demand, good air quality in the ClaZ, high yields or high crop growth efficiency in the greenhouse, and compares them with the baseline scenario. The results of the 350 simulation runs for the SRC sensitivity study are constrained to limiting the combined energy use intensity of the greenhouse and classroom to 250 kWh/m^2, and the CO_2 levels in the classroom are

Table 4. Input and output parameters for five scenarios: baseline, least energy demand, best air quality in the classroom, most crop yield, and most energy efficient crop yield.

Outputs	**Unit**	**Baseline**	**Least energy use**	**Highest air quality**	**Most crop yield**	**Most crop growth efficiency**
EUI of ClaZ	kWh/m^2/year	60.8	70.3	86.9	49.9	56.2
EUI of GZ	kWh/m^2/year	259.8	71.0	364.7	335.6	154.4
EUI_{tot} (GZ+ClaZ)	kWh/m^2/year	160.3	**70.6**	225.8	192.8	105.3
Mean daily density of plants (GZ)	g/m^2/day	146.4	142.3	141.6	160.2	146.8
Mean daily CO_2 (ClaZ)	ppm	904.7	950.4	**781.0**	1086.6	1112.1
Total fresh matter harvested	tDM/year	3.4	0.5	2.3	**7.6**	5.9
Crop growth efficiency	gFW/kWh/year	60	13	21	78	**110**
Annual building energy use	kWh/m^2/year	139.05	**133.13**	143.97	141.03	**135.28**
Input parameters						
Shade transmittance	-	50%	6%	29%	11%	29%
Rooftop window area	-	50%	71%	78%	89%	81%
Air mixing CorZ-GZ	-	50%	87%	2%	74%	65%
Air mixing GZ-ClaZ	-	50%	44%	0%	86%	100%
Heating setpoint	°C	16	15.3	16.4	16.8	15.8
Cooling setpoint	°C	27	28.7	27.0	27.5	28.6
Planted area	m^2	50%	8%	33%	94%	90%

limited to 1500 ppm to maximum two hours per day, as per school building guidelines.

If the designer wanted to achieve high yields, 7.6 tonnes of fresh lettuce could be grown per year with a total planted area (94%), with an EUI of 335.6 kWh/m^2 in the Greenhouse Zone. At an average consumption of lettuce per head of 6 kg/year (USDA 2017), this corresponds to the total lettuce consumption of 1222 people, 1.4 times the number of students in the school building. This requires a rooftop window size of 78% of the zone area, with shading in summer. Some heating is needed for this result, and cooling was triggered at 27 °C. Crops could be grown more energy efficiently, with less cooling and heating and significant air mixing to the ClaZ to compensate for energy use in the GZ. The combined EUI of the GZ ans ClaZ would thus drop from 192.8 to 105.3 kWh/m^2, and harvest would decrease to the still substantial rate of 5.9 tFW/year, in line with best practice values for lettuce greenhouses in the UK of 131 kWh/m^2 (The Carbon Trust 2012). This would be a significant improvement on the UK average indoor lettuce growth, with typical energy consumption of 230 kWh/m^2, and represent 4.8 times more growth per unit area (33 t/ha for protected lettuce farming in the UK) (Defra 2020).

On the other hand, optimal air quality in the classroom has a high energy cost due to the large amount of ventilation required, increasing the building energy demand by 10%. Air mixing to the classroom was not beneficial despite plants in the greenhouse acting as an "air purifier". However, the least energy use case shows that a successful building integrated greenhouse need not be energy intensive. Ventilating the classroom with greenhouse air rather than outdoor air 44% of the time would also decrease energy consumption, while keeping the air quality at its threshold limits. The EUI of the greenhouse and classroom zones combined was thus 70.6 kWh/m^2, and the total

amount of lettuce grown was 0.5 tFW/year.

The effect of including the GZ on the total building energy use was not significant. As seen in Section 2, a passive GZ provides a small buffer effect, reducing building energy demand by 1% compared with case with no greenhouse at all (131.1 kWh/m^2). However, running a greenhouse with the baseline input parameters would increase building energy demand by 5%. On the other hand, modifying the input parameters to the "Most crop growth efficiency" scenario, only increased the building energy demand by 3%. Using the input parameters for the "Most crop growth efficiency" scenario to produce the same greenhouse design placed on the ground rather than as BIA, would increase the greenhouse's EUI to 298 kWh/m^2. For the same yields, energy demand for a standalone greenhouse would thus be double, highlighting the benefits of the integration of the greenhouse to the building design. Past BIA models had focused on Mediterranean climates (Muñoz-Liesa et al. 2020), but the large demand for heating in more temperate climates such as in the UK highlights the large potential for heat recovery in different settings.

Further analysis would be required to find the optimally coupled configuration. These results can inform an optimisation with an appropriate cost function by proposing a limited set of sensitive variables. However, as the constraints of an optimisation would be building specific, it exceeds the scope of this work.

6. Conclusions

Research outcomes

The aim of this study was to quantify the trade-offs of integrating a greenhouse in symbiosis with a building through a novel co-simulation. Tested on an archetype of a school building in London, our co-simulation methodology enabled modelling the dynamic effect of plants on the ambient environment. The results are especially relevant across three aspects: using BES models for greenhouse HVAC sizing, the seasonal potential of reusing building "waste resources", and comparing trade-offs across objectives.

Firstly, by running the GES-II and BES models in an independent, yet interconnected way, it is possible to analyse the effect of the planted area on the temperature, humidity and CO_2 levels in the zone of interest. By feeding back this effect at each timestep of the simulation, different HVAC measures can be tested within the BES model to meet the needs of the greenhouse (e.g. through natural ventilation or dehumidification). This method could be used by architects and civil engineers seeking to add hydroponic farming to their building design and understand the effect of high-density plants on the building physics.

Secondly, a sensitivity analysis (SA) was performed to test the influence of seven input parameters on the outcome of the combined building-greenhouse model, in terms of energy use, air quality and crop yields. The two methods used highlighted the potential of reusing the air from the building to increase crop yields and decrease energy use. A seasonal breakdown of the SA results could inform further operational efficiencies. For instance, a large rooftop window will provide large yields but will increase the demand for cooling in summer due to high transpiration rates.

Finally, we identified four model outcomes which respond to four different school objectives. The design with highest crop harvest could potentially feed 1.4 times the student body, increasing building energy use by 8% compared with a building without

a greenhouse. If the aim of this school building is to achieve the most energy efficient crop yields, a design with significant air mixing could produce 6 tonnes of lettuce a year while only increasing the school building's energy consumption by 3%.

Further research

Whilst the co-simulation method was implemented on an archetype of a school building, it is applicable to any BIA setting and can be used to identify optimal configurations. The co-simulation uses validated building and greenhouse energy simulations, but the integrated model is not calibrated against a real-life BIA, as there were no known examples matching those conditions in the UK at the time of writing. Future work will investigate specific school buildings in London, UK to ascertain the potential of rooftop greenhouses based on individual school building design and tailor the optimisation to the objectives of the stakeholders (low energy use, thermal comfort, high crop growth, or simply educational). This would also offer the opportunity to further develop the model to include economic and societal impacts.

Depending on future objectives of school designs (and further larger buildings), this method can be used to optimise for air quality, food production in buildings, and reuse of "wasted" resources. As the trend towards BIA continues to grow, this co-simulation methodology can be used for larger scale application. The pandemic sweeping the world at the time of writing is sparking many conversations about the use of derelict spaces in city centres. As remote working becomes increasingly the norm, large swathes of space in office buildings and their dependent businesses might require repurposing. Perhaps, in an age of increasing awareness of the source of food, climate change and economic initiatives for resource use efficiency, this will also provide an ideal opportunity to foster building integrated agriculture.

Acknowledgement(s)

We would like to thank Willy Bernal and Qipeng for their help with Energy Plus and MLE+. Further thanks to Kathryn Menberg for assisting with understanding sensitivity studies for building energy models.

Funding

This work was supported by the Engineering and Physical Sciences Research Council grant EP/L016095/1. The authors also acknowledge the support of AI for Science and Government (ASG), UKRI's Strategic Priorities Fund awarded to the Alan Turing Institute, UK (EP/T001569/1) and the Centre for Digital Built Britain within the Construction Innovation Hub (CIH).

Nomenclature

Physics Constants

c_p	Heat capacity of air at 25°C	$1003.2\,\mathrm{J/kg/K}$
h_{fe}	Latent heat of vaporisation of water	$2.441 \times 10^{-6}\,\mathrm{J/kg}$
M_{CH_2O}	Molar mass of CH_2O	$0.03\,\mathrm{kg/mol}$

M_{CO_2}	Molar mass of CO_2	0.044 kg/mol
Abbreviations		
BIA	Building Integrated Agriculture	
BES	Building Energy Simulation	
GES	Greenhouse Energy Simulation I	
GES-II	Greenhouse Energy Simulation II	
GZ	Greenhouse Zone	
ClaZ	Middle Floor south facing Classroom Zone	
CorZ	Top Floor Corridor Zone	
SH	Sensible Heat	W
LH	Latent Heat	W
ACH	Air change per hour	/h
DM	Dry matter weight of crop	kg/m^2
EUI	Energy Use Intensity	kWh/m^3
FW	Fresh weight of crop (including water content)	kg
SRC_i	Standard Regression Coefficient of parameter i	
μ_i^*	Absolute mean of Elementary Effect of parameter i	
Equation terms		
ΔCO_2	Change in CO_2 output from GES-II	m^3/s
ΔLH	Change in Latent Heat output from GES-II	W
ΔSH	Change in Sensible Heat output from GES-II	W
ΔT	Timestep of GES-II and BES	900 s
E_{ClaZ}	Annual energy demand of the ClaZ for HVAC	kWh
E_{GZ}	Annual energy demand of the GZ for HVAC	kWh
MC	Mass flow of carbohydrates in GES-II	$kg/m^3/s$
Q_{conv}	Sum of convective heat transfer from surfaces in GZ in BES	W
$q_{CorZ \to GZ}$	Volume flow rate of air from CorZ to GZ	m^3/s
$q_{GZ \to ClaZ}$	Volume flow rate of air from GZ to ClaZ	m^3/s
Q_{HVAC}	Heat transfer from HVAC system in GZ in BES	W
Q_{inf}	Heat transfer due to infiltration of outside air in GZ in BES	W
$Q_{int\ loads}$	Sum of convective internal loads	W
QP	Latent heat flow GES-II and BES	W
QV	Sensible heat flow in GES-II and BES	W
T_{CorZ}	Temperature of internal air in CorZ in BES	°C
W_{CorZ}	Air moisture content of internal air in CorZ in BES	kg/m^3
W_{GZ}	Air moisture content of internal air in GZ in BES	kg/m^3
A_{ClaZ}	Area of ClaZ	$252\,m^2$
A_{GZ}	Area of GZ	$252\,m^2$
V_{GZ}	Volume of GZ	$756\,m^3$
ρ_i	Density of internal air in GZ in GES-II	kg/m^3
C_i	CO_2 concentration of internal air in GZ in GES-II	ppm
T_f^{GES-II}	Temperature of floor in GZ in GES-II	°C
T_i	Temperature of internal air in GZ in GES-II	°C
T_m	Temperature of irrigation mat in GZ in GES-II	°C
T_t	Temperature of hydroponics tray in GZ in GES-II	°C
T_v	Temperature of vegetation in GZ in GES-II	°C
W_i	Air moisture content of internal air in GZ in GES-II	kg/m^3
ρ_{GZ}	Density of inter air in GZ in BES	kg/m^3
C_{GZ}	CO_2 concentration of internal air in GZ in BES	ppm
T_f^{BES}	Temperature of floor in GZ output from BES	°C

T_{f0}^{BES}	Temperature of floor in GZ without rooftop window in BES	°C
T_{GZ}	Temperature of internal air in GZ in BES	°C

7. Disclosure statement

There are no competing interests to declare.

8. Data availability statement

Data can be made available upon request to the corresponding author. The code is available for reproduction on GitHub. The multiple co-simulation files can be generated with Jans-Singh (2020) and a reproducible example of the co-simulation can be found at Jans-Singh (2021).

9. Supplementary information

Table 5 contains the summary statistics for 3309 schools in Central London, obtained by merging data from DEC, postcode data and National Statistics for schools (DfE 2018).

Appendix A. Crop growth model

This section describes the detailed equations of the Greenhouse Model. There are three main components to the model: (1) Absorption of the radiation by the plants, (2) Crop transpiration, (3) Crop photosynthesis. The other main flows in the greenhouse are conduction and convection flows in between each of the nodes illustrated in Figure 4, but as they are the same as described in equations 9 they will not be detailed here.

A.1. *Solar radiation*

The solar radiation absorbed by the plant canopy is computed from the direct radiation transmitted through the window[5], and the diffuse radiation which is reflected back from the floor surfaces (Equation (A1)). The transmitted solar radiation is calculated from the transmission properties of the windows in EnergyPlus: the exterior windows are 3 mm clear glass, while the rooftop window has double glazing and shading applied when temperatures surpass 28 °C in the greenhouse zone. Equation (A1) further shows how the transmitted solar radiation reaching the canopy is further divided between PAR (photosynthetically active radiation) and NIR (near-infrared radiation), which are assumed to be half according to Monteith and Unsworth (2008) as the leaves are assumed to be black bodies (close to reality for the visible spectrum). The leaves are represented as cylindrical bodies which shade the lower leaves, thus the absorbed radiation is calculated geometrically with the incidence angle of the sun (its azimuth and elevation). The model used was adapted from De Zwart (1996).

[5]Superscrifts r and f refer to direct and diffuse radiation respectively.

Table 5. Summary statistics for 3309 schools in Central London, from merging DEC and National Statistics for schools datasets.

School characteristic	Statistic	Independent school	State-funded primary	State-funded secondary	State-funded special school	Source
Number of schools	Total in Greater London	563	1813	483	135	Combined
Total EUI (kWh/m^2)	Median of all buildings	168.5	174.6	172.6	211.0	DEC
	(Best pratice)	135.3	148.0	150.0	174.7	DEC
Electricity EUI (kWh/m^2)	Median	61.1	51.1	64.4	62.9	DEC
	Best practice	48.3	40.0	50.1	49.0	DEC
Thermal EUI (kWh/m^2)	Median	114.7	129.5	116.2	153.6	DEC
	Best practice	76.8	99.0	89.0	113.0	DEC
Weighted EUI (kWh/m^2)	mean weighted by inspection date	178.1	185.6	185.2	222.0	DEC
Total floor area (m^2)	Mean	3361	3017	10943	3542	DEC
Headcount	Mean	342	426	1096	106	NatStats[4]
Number of buildings in school complex	Mean	1.4	1.4	2.3	1.4	Combined
Inspection counts	Mean	2.5	4.3	4.2	4.1	DEC
Change in EUI from first inspection (kWh/m^2)	Mean	-6.8	-20.7	-22.4	-21.1	DEC
Presence of air conditioning	Most repeated	No	No	Yes	No	DEC
	Percentage of total	36%	36%	59%	42%	DEC
Type of building environment	Most repeated	Heating and Natural Ventilation				
	Percentage of total	88%	94%	77%	81%	DEC
DEC Operational Rating Band	Most repeated	F	D	E	E	DEC
	Percentage of total	29%	37%	33%	31%	DEC
Main heating fuel	Most repeated	Natural Gas	Natural Gas	Natural Gas	Natural Gas	DEC
	Percentage of total	94%	98%	96%	98%	DEC
Pupils taking a free school meal	Total number of children	0	92,719	60,436	6512	DEC
	Mean percentage in school	-	14%	15%	36%	NatStats

$$QS_v = PAR_v^r + PAR_v^f + NIR_v^r + NIR_v^f. \quad \text{(W)} \quad \text{(A1)}$$

The direct (Equation (A2)) and diffuse (Equation (A3)) PAR directly absorbed by the canopy is described by negative exponential decay of light with LAI in a homogeneous crop:

$$PAR_v^r = PAR^r(1-\rho_v)(1-e^{-K_r^{PAR}LAI}), \quad \text{(W)} \quad \text{(A2)}$$
$$PAR_v^f = PAR^f(1-\rho_v)(1-e^{-K_f^{PAR}LAI}). \quad \text{(W)} \quad \text{(A3)}$$

The extinction coefficients K_r^{PAR} and K_f^{PAR} are assumed to be the same and equal 0.7. ρ_v is the reflection coefficient of the canopy of PAR, here set to 0.35 (Vanthoor 2011).

$$K_f^{PAR} = 0.85, \quad \text{(A4)}$$
$$K_r^{PAR} = 0.88 + 2.6e^{-0.18\alpha}. \quad \text{(A5)}$$

The crops reflect considerably more NIR: back to the greenhouse window, scattered through its leaves, and to greenhouse surfaces, which may reflect back again to the crops. The reflection and transmission coefficients are computed using vector algebra from the angle of incidence α of solar radiation at the given time, which can be calculated geometrically from the date, time, azimuth and elevation of the sun (De Zwart 1996).

$$NIR_v^r = NIR^r(0.67 - 0.06e^{-0.08\alpha} - (0.68 - 0.5e^{-0.11\alpha})e{-}K_r^{NIR}LAI), \quad \text{(W)} \quad \text{(A6)}$$
$$NIR_v^f = NIR^f(0.65 - 0.65e^{-K_f^{NIR}LAI}). \quad \text{(W)} \quad \text{(A7)}$$

The extinction coefficients are given by:

$$K_f^{NIR} = 0.27, \quad \text{(A8)}$$
$$K_r^{NIR} = 0.25 + 0.38e^{-0.12*\alpha}. \quad \text{(A9)}$$

The total PAR absorbed by the canopy is also essential for the photosynthesis equation, where it is expressed in photosynthetic photon flux density (PPFD) at the wavelength of λ =550 nm.

$$PPFD_v = \frac{PAR_v^r + PAR_v^f}{h\frac{c}{\lambda}N_A}, \quad (\mu\text{mol/m}^2\text{/s}) \quad \text{(A10)}$$

where N_A is Avogadro's constant ($6.022 \times 10^{23}\,\text{mol}^{-1}$), h is Planck's constant ($6.663 \times 10^{-34}\,\text{J/s}$) and c is the speed of light ($2.998 \times 10^{17}\,\text{nm/s}$).

A.2. *Transpiration*

Transpiration is one of the main effects of the plant module; the process of water evaporation from small pores on the leaf surface called stomata, in response to photosynthesis. This varies with the leaf area index (LAI), and solar radiation. As explained earlier, solar radiation is transferred directly from the BES model, and varies with window size, day of year, and shading.

LAI on the other hand varies with growth rate of leaf and the specific leaf index (SLA). Indeed $LAI = SLA \times C_{leaf}$. The SLA of lettuce is given as $35\,\mathrm{m}^2/\mathrm{kg}$.

Transpiration T is a function of the difference in moisture content at the plant surface W_v and the internal air W_i, the LAI, the latent heat of vaporisation of the air h_{fe}, and r_a and r_s the aerodynamic and stomatal resistance to vapour transfer respectively (s/m) (Graamans et al. 2017).

$$T = AF_g A_v 2\ LAI\ h_{fe} \frac{(W_v - W_i)}{r_a + r_s}. \qquad \text{(W)} \quad \text{(A11)}$$

The stomatal resistance is calculated based on the photosynthetic photon flux density, defined as the photon flux density of PAR (PPFD in $\mu\mathrm{mol}/\mathrm{m}^2/\mathrm{s}$).

$$r_a = 100\ or\ 200 \quad \text{(if forced air circulation is on/off)}, \qquad \text{(s/m)} \quad \text{(A12)}$$

$$r_s = 60 \frac{1500 + PPFD_v}{200 + PPFD_v}. \qquad \text{(s/m)} \quad \text{(A13)}$$

A.3. *Crop growth, photosynthesis and respiration*

Photosynthesis is not directly dependent on humidity, provided there is sufficient water supply to the roots, and also does not appear to be significantly dependent on the crop type (Vanthoor 2011). Future developments of the model could however include inhibition factors due to excess humidity causing mould on the plants.

The crop growth model for lettuces used here follows the tomato yield model by Vanthoor (2011), adapted for microgreens in Ward, Jans-Singh, and Choudhary (2018) for a hydroponic farm, and here for growing lettuces in a semi-commercial school greenhouse. It is structured as a carbohydrate buffer and distribution model, where the buffer (C_{buf}) stores the carbohydrates produced through photosynthesis and maintenance respiration, and distributes the carbohydrates to its plant organs (C_{leaf} and C_{stem}) when the temperatures allow. These are measured in kg of carbohydrate CH_20 by area. This flow of carbohydrates is influenced by the actual temperature (T_v), the mean and sum of the plant temperature over the last 24 hours (T_v^{24} and T_v^{sum}). LAI is a semi-state of the model as it increases proportionally to C_{leaf}. When the LAI exceeds its maximum value (6 in our case), the leaves are pruned back to 5% of their size, which allows an approximation of the accumulated amount of harvested dry matter. Essentially, the crop growth model is inhibited by temperature, and its respiration and photosynthesis components are inhibited or promoted through solar radiation, LAI and CO_2 concentration.

Although the complete model is too complex to be fully included here, this section will define the main equations for photosynthesis by presenting the calculations for the leaf organ. The list of model parameters and associated symbols is inluded in table A2.

The change in mass of leaves over a timestep is defined by Equation (A14).

$$\frac{dC_{leaf}}{dt} = MC_{buf\rightarrow leaf} - MC_{leaf\rightarrow air} - MC_{leafharvested}, \qquad (\mathrm{kg/m^2/s}) \quad \text{(A14)}$$

where $MC_{buf\rightarrow leaf}$ denotes the flow from the buffer to the leaf, $MC_{leaf\rightarrow air}$ corresponds to the maintenance respiration of the leaves and $MC_{leafharvested}$ is the dry matter harvested in the timestep (all in $\mathrm{kg/m^2/s}$), and maintenance respiration in The flow of carbohydrates from the buffer to the leaf corresponds to the photosynthesis process and is defined in Equation A15. The maintenance respiration, with flow from the leaves to the air, is defined in Equation A16. Their variation with temperature and the amount available in the buffer (C_{Buf}) is illustrated in Figure A1.

$$MC_{buf\rightarrow leaf} = h_{temp} h_{buf} g_t \; g_{leaf}, \qquad (\mathrm{kg/m^2/s}) \quad \text{(A15)}$$

$$MC_{buf\rightarrow air} = r_{leaf} MC_{buf\rightarrow leaf} + r_{stem} MC_{buf\rightarrow stem}, \qquad (\mathrm{kg/m^2/s}) \quad \text{(A16)}$$

where r is the respiration rate and g is the growth rate of the plant organs denoted by their subscript.

As mentioned before, respiration and photosynthesis are inhibited by air temperature and the amount available in the buffer, as shown in Figure A1. The temperature inhibition factor h_{temp} was calculated based on four cardinal temperatures from Boote and Scholberg (2006). Beyond a temperature T_{base} and T_{max} no flow of carbohydrates is expected ($h_{temp} = 0$), and it is optimal ($h_{temp} = 1$) between two temperature points T_{opt1} and T_{opt2} (Figure A1). The relationship in between is assumed to be linear. Carbohydrate flow is also limited by the amount available in the buffer, where $h_{buf} = 1$ when there are sufficient carbohydrates available ($C_{buf}^{min} < C_{buf} < C_{buf}^{max}$). As growth rate increases with temperature, the growth rate at 20 °C g_{leaf} is multiplied by the growth rate dependency on temperature g_t (de Koning 1994), for its validated range between 17 and 23 °C, beyond which it is restricted with the growth inhibition factors. The differentiatable form of these equations is taken from Vanthoor (2011).

$$g_t = 0.048 \times T_v^{24} + 0.06, \qquad \text{(A17)}$$

$$h_{buf} = \begin{cases} 1, & \text{if } C_{buf}^{min} < C_{buf} < C_{buf}^{max} \\ 0, & \text{otherwise} \end{cases} \qquad \text{(A18)}$$

$$h_{temp} = \begin{cases} 1, & \text{if } T_{opt}^{1} < T_v^{24} < T_{opt}^{2} \\ 0, & T_{base} < T_v^{24} < T_{max} \end{cases} \qquad \text{(A19)}$$

The amount of carbohydrates available in the buffer depends on the net photosynthesis rate A_n A20.

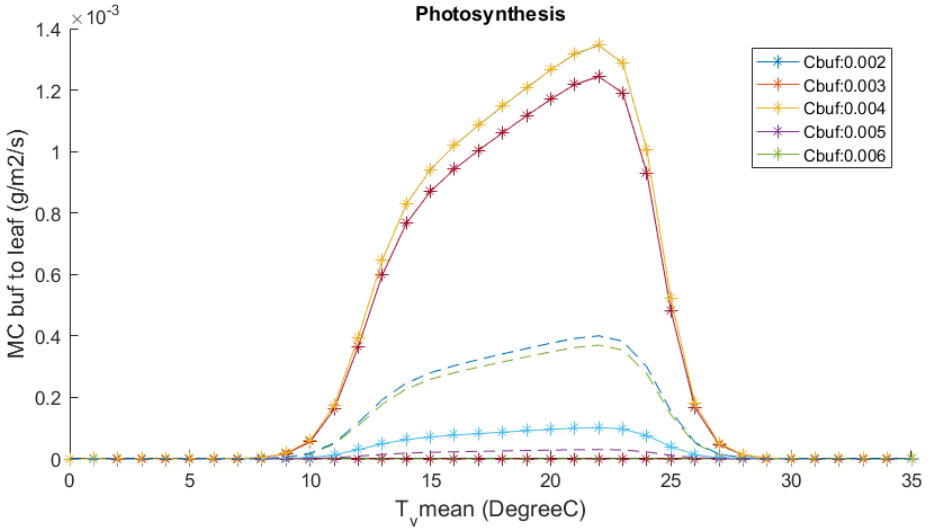

Figure A1. Flow of CH_20 from the buffer to the leaf $MC_{buf \to leaf}$ (straight line), and from the leaf to the air $MC_{leaf \to air}$ (dotted line, maintenance respiration).

$$MC_{air \to buf} = M_{CH_20}\, h_{buf}(A_n), \qquad (\mathrm{kg/m^2/s}) \quad \text{(A20)}$$

where M_{CH_20} is the molar mass of carbohydrates. A_n is the difference between the gross canopy photosynthesis rate P, and mitochondrial respiration during light-time R_d. These processes are limited by the saturation of the leaves, represented through the inhibition factor h_{buf}.

Photosynthesis occurs in the chloroplasts of leaves, cells containing stomata, a gel-like substance containing an enzyme called Rubisco, which converts CO_2 to carbohydrates. This process is called carboxylation, and is modelled through three limiting states: A_c limited by CO_2 and the Rubisco enzyme (Figure 2(c)), A_j limited by light and electron transport (Figure 2(b)), and A_s limited by accumulating starch at the chloroplast (Figure 2(c)) (Farquhar, von Caemmerer, and Berry 1980; Von Caemmerer 2013; Bonan 2015).

$$A_n = min(A_c, A_j, A_s) - R_d, \qquad (\mathrm{\mu mol/m^2/s}) \quad \text{(A21)}$$

where A_n is the carbon assimilation rate and R_d is the maintenance respiration rate.

$$R_d = min(A_c, A_j, A_s)\frac{\Gamma}{c_i}, \qquad (\mathrm{\mu mol/m^2/s}) \quad \text{(A22)}$$

The Rubisco-limited rate of photosynthesis A_c $\mu\mathrm{mol}\{CO_2\}/\mathrm{m^2/s}$ is given by:

$$A_c = \frac{V_{cmax}(c_i - \Gamma)}{c_i + K_C(1 + o_i/K_O)}, \qquad (\mathrm{\mu mol/m^2/s}) \quad \text{(A23)}$$

where K_c and K_O are the Michaelis-menten constants for carboxylation and oxygenation of Rubisco respectively. V_{cmax} is the maximum rate of carboxylation (Equa-

tion (A30)). The rate of carboxylation is assumed to be equal to the maximum rate of carboxylation in this model.

The electron transport limitation rate is:

$$A_j = \frac{J(c_i - \Gamma)}{4(c_i + 2\Gamma)}. \qquad (\mu mol/m^2/s) \quad (A24)$$

J is the rate of electron transport, taken from Farquhar, von Caemmerer, and Berry (1980), as the smallest of the roots to the following equation:

$$\theta J^2 + (J_{max} + \alpha * PAR)J + (\alpha J_{max} PAR), \qquad (A25)$$

where J_max is t

The third limiting state lies in the plant's ability to utilise the products of photosynthesis of starch and sugar, and is known as the triose phosphate limitation rate which is given by:

$$A_s = V_{cmax}/2. \qquad (\mu mol/m^2/s) \quad (A26)$$

Here, c_i is the CO_2 concentration (umol/mol) at the site of CO_2 fixation in the chloroplast, taken to be 90% of air CO_2 concentration levels (Bonan, 2013). Γ is the CO_2 compensation point, calculated from the oxygen partial pressure in the chloroplast (Equation (A27)). τ is the CO_2O2 specificity ratio for Rubisco from Table A1 (Collatz et al. 1991), which is dependent on temperature.

$$\Gamma = o_i/(2\tau). \qquad (Pa) \quad (A27)$$

Several of the parameters above depend on temperature. The kinetic constants K_o, K_c and τ are calculated using the Q10 function in Collatz et al. (1991).

$$k = k_{25} Q_{10}^{(T_i - 25)/\Delta T}, \qquad (A28)$$

where k_{25} is the parameter value at 25 °C and Q_{10} is the relative change in the parameter for a ΔT change in temperature. The 25 °C constants are summarised in Table A1.

Table A1. Temperature varying parameters for Equation A28

	k_{25}	Q_{10}	ΔT
K_c	30 Pa	2.1	10 °C
K_o	30 000 Pa	1.2	10 °C
τ	2600	0.57	10 °C

The most sensitive parameters for this model are J_{max} and V_{cmax}. There exists a strong relationship between these two variables as they represent the resource allocation between the two photosynthetic cycles – electron transport and the Calvin–Benson cycle. Since these vary with temperature (Bonan 2015; Walker et al. 2014), we used the time varying equation in Vanthoor (2011) for J_{max} (Eq. A29), and the relationship of V_{cmax} with J_{max} from Fan, Zhong, and Zhang (2011) (Eq. A30).

$$J_{max} = J_{max}^{25} e^{E_j \frac{T_v - T_{25,K}}{RT_v T_{25,K}}} \frac{1 + e^{\frac{ST_{25,K} - H}{RT_{25,K}}}}{1 + e^{\frac{ST_v - H}{RT_v}}}, \qquad (\mu\text{mol/m}^2\text{/s}) \quad \text{(A29)}$$

where E and H are the activation and deactivation energy, and S is the slope of J_{max}'s relationship with temperature (Vanthoor 2011).

$$V_{cmax} = J_{max}/1.64. \qquad (\mu\text{mol/m}^2\text{/s}) \quad \text{(A30)}$$

The effect of the three limitation rates on carbon assimilation (A_n) is shown in Figure A2. Mean ambient conditions are set to 400 ppm, 25 °C and 5000 W of solar radiation on the plant canopy. Varying A_n with visible radiation reveals the proportional relationship with light, where A_n can reach 8.2 µmol/m^2/s when 12 000 W of solar radiation reaches the plant canopy. A_n increases rapidly with CO_2 levels under 400 ppm, but the effect of additional CO_2 tapers around 1000 ppm, where $A_n = 8.2$ µmol/m^2/s. Carbon assimilation peaks with this model at 10 °C to 4.7 µmol/m^2/s with the given mean conditions of CO_2 and light.

The potential fruit growth rate coefficient used in Vanthoor (2011) was 2.6 mg/m^2/s, from which growth rates of other plant organs and plant respiration rates were derived. To adapt our model to lettuce growth, we decided to base the growth rate on the yield of Growing Underground (Ward, Jans-Singh, and Choudhary 2018), which was approximately 2 kg/m^2/20 days in ideal conditions (at 20 °C), which gave a total growth rate of 1.6 mg/m^2/s, in line with values from Van Iersel (2003). The max LAI of 6 was found from Slamet et al. (2017) and Tei, Scaife, and Aikman (1996). The SLA was chosen as 35 m^2/kg from a mean of literature values (Lee and Heuvelink 2003; Galieni et al. 2016). Pruning was assumed to happen continuously once C_{leaf} surpassed LAI/SLA = 170 g/m^2. To solve the discontinuity the solver is stopped and reinitialised with the following conditions (called an event function in MATLAB). Equation (A33) shows the newly initialised values post harvesting at time $t = h + 1$, where $t = h$ is the harvest time reached when $C_{leaf} = C_{leaf}^{max}$. All units are in kg/m^2.

$$C_{leaf}^{t=h+1} = 0.05 \times C_{leaf}^{max}, \qquad (\text{kg/m}^2) \quad \text{(A31)}$$

$$C_{leaf\ harvested}^{t=h+1} = 0.95 \times C_{leaf}^{max}, \qquad (\text{kg/m}^2) \quad \text{(A32)}$$

$$C_{stem}^{t=h+1} = 0.2 \times C_{stem}^{t=h}. \qquad (\text{kg/m}^2) \quad \text{(A33)}$$

The total harvested amount of leaves is referred to as the Dry Matter (DM in kg/m^2). The fresh weight (FW) of harvested lettuce is calculated from the dry matter weight, with η the conversion parameter, taken as the average from Fu (2008); Gent (2012).

$$\text{FW} = \eta \text{DM}. \qquad (\text{kg/m}^2) \quad \text{(A34)}$$

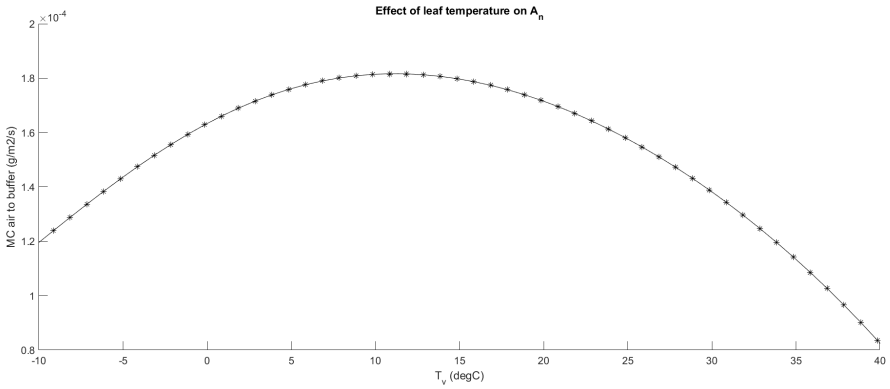

(a) Varying temperature of plant

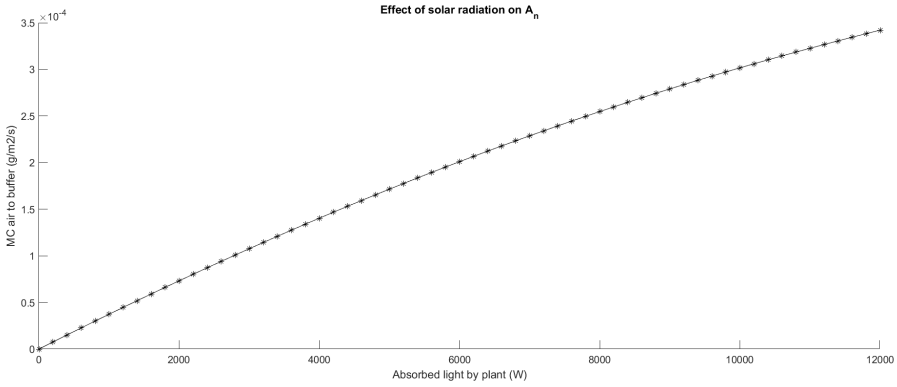

(b) Varying incoming solar radiation

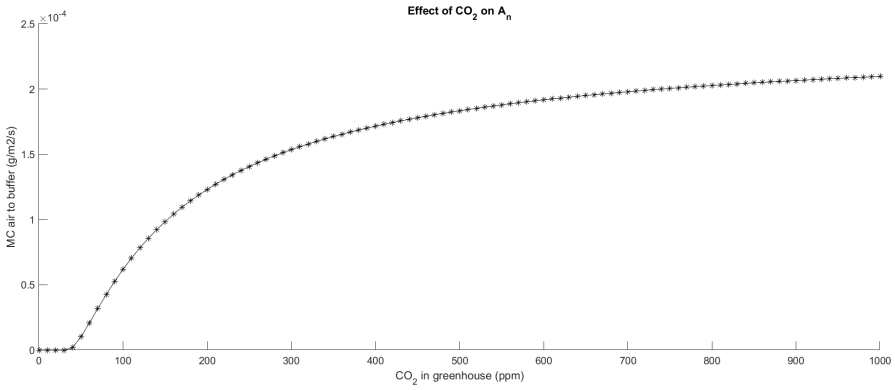

(c) Varying CO_2

Figure A2. Variation of amount of carbohydrates available in the buffer. With $h_{buf=1}$, it is equivalent to the variation in carbon assimilation rate A_n.

Table A2.: Input parameters and nomenclature for the GES-II model

Input	Annotation	Number	Unit	Source
Physics constants				
Avogadro's constant	N_A	6.02E+23	mol^{-1}	-
Planck's constant	h	6.66E-34	J/s	-
Speed of light	c	3.00E+17	nm/s	-
Mean wavelength	λ	5.50E+02	nm	(Davis 2015)
Environmental conditions in the GES-II				
Internal air temperature	T_i		°C	-
Moisture content of the internal air	W_i		kg/m^3	-
CO_2 concentration of the internal air	C_i		ppm	-
Temperature of the plant canopy	T_v		°C	-
Moisture content of the plant canopy	W_v		kg/m^3	-
Radiation model				
Total solar radiation absorbed by the vegetation	QS_v		W	-
Direct visible radiation absorbed by the vegetation	PAR_v^r		W	-
Diffuse visible radiation absorbed by the vegetation	PAR_v^f		W	-
Direct Near infrared radiation absorbed by the vegetation	NIR_v^r		W	-
Diffuse Near infrared radiation absorbed by the vegetation	NIR_v^r		W	-
Extinction coefficient (x is for direct or diffuse, y is for PAR or NIR)	K_x^y		-	De Zwart (1996)
Leaf area index	LAI		-	-
Photosynthetic photon flux density reaching canopy	$PPFD_v$			-
Transpiration model				-
Fraction of growth	AF_g	0.9	-	Vanthoor (2011)
Latent heat of vaporisation of water at 20°C	h_{fe}	2437000	J/kg	-
Transpiration rate	T		W	Stanghellini and van Meurs (1992)
Area of vegetation	A_v		m^2	-
Aerodynamic resistance	r_a		s/m	Graamans et al. (2017)
Stomatal resistance	r_s		s/m	Graamans et al. (2017)
Crop growth model				
Mass of carbohydrates of leaf	C_{leaf}		$kg/m^2/s$	-
Mass flow rate from buffer to leaf	$MC_{buf \rightarrow leaf}$		$kg/m^2/s$	-
Maintenance respiration rate of leaf	$MC_{leaf \rightarrow air}$		$kg/m^2/s$	-
Harvest rate	$MC_{leaf \rightarrow harvested}$		$kg/m^2/s$	-

Table A2 continued from previous page

Input	Annotation	Number	Unit	Source
Mass flow rate from buffer to stem	$MC_{buf \rightarrow stem}$		kg/m^2/s	-
Temperature inhibition factor for leaf growth	h_{temp}		-	Vanthoor (2011)
Buffer inhibition factor for leaf and stem growth	h_{buf}		-	Vanthoor (2011)
Temperature growth rate between 17 and 23 °C	g_t		-	de Koning (1994)
Growth rate of leaf in optimal conditions	g_{leaf}	1.27E-06	kg/m^2/s	Assumed, see text
Respiration rate of stem in optimal conditions	r_{stem}	7.40E-08	kg/m^2/s	Vanthoor (2011)
Respiration rate of leaf in optimal conditions	r_{leaf}	1.27E-06	kg/m^2/s	Vanthoor (2011)
Base temperature for crop growth model	T_{base}	10	°C	Boote and Scholberg (2006)
Maximum temperature for crop growth model	T_{max}	34	°C	Boote and Scholberg (2006)
First optimal temperature model	T^1_{opt}	12	°C	Boote and Scholberg (2006)
Second optimal temperature model	T^2_{opt}	24.5	°C	Boote and Scholberg (2006)
Mean 24 hour temperature of the plant	T^{24}_v		°C	Vanthoor (2011)
Maximum buffer capacity per unit area of cultivated floor	C^{max}_{buf}	0.8	kg/m^2/s	Vanthoor (2011)
Minimum buffer capacity per unit area of cultivated floor	C^{min}_{buf}	0.04	kg/m^2/s	Vanthoor (2011)
Molar mass of CH20	MCH_20	0.03	kg/mol	-
Molar mass of CO_2	MCO_2	0.044	kg/mol	-
Specific leaf area	SLA	35	m^2/kg	Average from Lee and Heuvelink (2003); Galieni et al. (2016)
Dry matter harvest mass	$C_{leaf\ harvest}$	0.1714	kg/m^2	-
Max LAI at harvest	LAI_{max}	6	-	Tei, Scaife, and Aikman (1996)
Cumulative harvested dry matter	DM		kg/m^2	-
Fresh weight of harvested crop	FW		kg/m^2	
Ratio of DM:FW	η	8	-	Average from Fu (2008); Gent (2012)
Carbon assimilation rate model				
Carbon assimilation rate model	A_n		µmol/m^2/s	

Table A2 continued from previous page

Input	Annotation	Number	Unit	Source
Rubisco limitation rate	A_c		µmol/m^2/s	
Electron transport limitation rate	A_j		µmol/m^2/s	
Triose phosphate (starch) limitation rate	A_s		µmol/m^2/s	
Maximum rate of carboxylation	V_{cmax}		µmol/m^2/s	Fan, Zhong, and Zhang (2011)
Rate of electron transport	J		µmol/m^2/s	
Maximum rate of electron transport	J_{max}		µmol/m^2/s	
Gas constant for J_{max} calculation	R	8.314	J/K/mol	Farquhar, von Caemmerer, and Berry (1980)
Slope for J_{max} calculation	S	710	J/K/mol	Farquhar, von Caemmerer, and Berry (1980)
Deactivation energy for J_{max} calculation	H	220000	J/mol	Farquhar, von Caemmerer, and Berry (1980)
Activation energy for J_{max} calculation	E	37000	J/mol	Farquhar, von Caemmerer, and Berry (1980)
Degree of curvature of electron transport rate	θ	0.7	-	Farquhar, von Caemmerer, and Berry (1980)
Fraction of incident absorbed PAR absorbed by leaves	α	0.385	mol{e}/mol{photon}	von Caemmerer (2013)
Electron transport rate at 25 °C	J_{max}^{25}	250	µmol/m^2/s	Vanthoor (2011)
Carboxylation rate at 25 °C	V_{max}^{25}	152.4390244	µmol/m^2/s	
CO_2 compensation point	Γ	-	Pa	Bonan (2015)
Partial pressure of O_2 in chloroplast	o_i	2.12E+04	Pa	Bonan (2015)
Partial pressure of CO_2 in chloroplast	c_i	$0.9C_i/10$	Pa	Bonan (2015)
Michaelis constant for carboxylation	K_c	-	Pa	Collatz et al. (1991)
Michaelis constant for oxidation	K_o	-	Pa	Collatz et al. (1991)
CO_2O_2 specificity ratio for Rubisco	τ	-	Pa	Collatz et al. (1991)

References

Benis, Khadija, Christoph Reinhart, and Paulo Ferrao. 2017. "Development of a simulation-based decision support workflow for the implementation of Building-Integrated Agriculture (BIA) in urban contexts." *Journal of Cleaner Production* 147: 589–602. http://www.sciencedirect.com/science/article/pii/S0959652617301452.

Benis, Khadija, Irmak Turan, C. F. Reinhart, and Paulo Ferrão. 2018. "Putting rooftops to use - A Cost-Benefit Analysis of food production vs. energy generation under Mediterranean climates." *Cities* 78: 166–179. http://www.hindawi.com/journals/scientifica/2013/528940/.

Bernal, W, M Behl, T Nghiem, and R Mangharam. 2014. "Campus-wide integrated building energy simulation." *2014 ASHRAE/IBPSA-USA Building Simulation Conference* (December): 227–234. https://www.scopus.com/inward/record.uri?eid=2-s2.0-84938845599&partnerID=40&md5=1a5623c7f62ce45232831bb4fe948060.

Blackman, F F. 1905. "Optima and Limiting Factors." *Annals of Botany* 19 (74): 281–295.

Bonan, Gordon. 2015. "Leaf Photosynthesis and Stomatal Conductance." In *Ecological Climatology*, 241–263. Cambridge: Cambridge University Press. /core/books/ecological-climatology/leaf-photosynthesis-and-stomatal-conductance/ABE07A1CC462A9F2ECFBB4BC3775468C.

Boote, K.J., and J.M.S. Scholberg. 2006. "Developing, parameterizing, and testing of dynamic crop growth models for horticultural crops." *Acta Horticulturae* 718 (718): 23–34. https://www.actahort.org/books/718/718_1.htm.

Both, A. J., L. D. Albright, and R. W. Langhans. 1998. "Coordinated management of daily PAR integral and carbon dioxide for hydroponic lettuce production." *Acta Horticulturae* 456: 45–51.

Boulard, Thierry, Jean Claude Roy, Jean Baptiste Pouillard, Hicham Fatnassi, and Ariane Grisey. 2017. "Modelling of micrometeorology, canopy transpiration and photosynthesis in a closed greenhouse using computational fluid dynamics." *Biosystems Engineering* 158: 110–133.

BRE. 2016. *National Calculation Methodology (NCM) modelling guide (for buildings other than dwellings in England)*. Technical Report. http://www.uk-ncm.org.uk/filelibrary/NCM_Modelling_Guide_2013_Edition_21October2016.pdf.

Brechner, Melissa, Aj Both, and Cea Staf. 1996. "Hydroponic Lettuce Handbook." *Cornell University CEA Program* 48.

Campolongo, Francesca, Jessica Cariboni, and Andrea Saltelli. 2007. "An effective screening design for sensitivity analysis of large models." *Environmental Modelling & Software* 22: 1509–1518. www.elsevier.com/locate/envsoft.

Capital Growth. 2016. *Reaping Rewards II - Measuring and valuing urban food growing*. Technical Report. London: Sustain. https://www.sustainweb.org/secure/ReapingRewardsII.pdf.

Coley, David A., and Alexander Beisteiner. 2002. "Carbon Dioxide Levels and Ventilation Rates in Schools." *International Journal of Ventilation* 1 (1): 45–52. http://www.tandfonline.com/doi/full/10.1080/14733315.2002.11683621.

Collatz, G. James, J. Timothy Ball, Cyril Grivet, and Joseph A. Berry. 1991. "Physiological and environmental regulation of stomatal conductance, photosynthesis and transpiration: a model that includes a laminar boundary layer." *Agricultural and Forest Meteorology* 54 (2-4): 107–136.

Davis, Phillip. 2015. *Lighting: the principles, Technical guide*. Technical Report. Stockbridge: Stockbridge Technology Centre. https://horticulture.ahdb.org.uk/sites/default/files/u3089/Lighting_The-principles.pdf.

DCLG. 2020. "Energy Performance of Buildings Data: England and Wales. Department for Communities and Local Government." London. https://epc.opendatacommunities.org/display/search.

de Koning, A. N. M. 1994. "Development and dry matter distribution in glasshouse tomato: a

quantitative approach." PhD diss., Agricultural University, Wageningen, The Netherlands.
De Zwart, H F. 1996. "Analyzing energy-saving options in greenhouse cultivation using a simulation model." PhD diss., Wageningen University.
Defra. 2020. *Food Statistics in your pocket: Global and UK supply.* Technical Report. London: Department for Environment Food and Rural Affairs. https://www.gov.uk/government/publications/food-statistics-pocketbook.
DES. 2019. "Information - Department of Education and Skills." (057). https://www.education.ie/en/Schools-Colleges/Information/Diversity-of-Patronage/Diversity-of-Patronage-Survey-of-Parents.html.
Despommier, Dickson. 2011. "The vertical farm: Controlled environment agriculture carried out in tall buildings would create greater food safety and security for large urban populations." *Journal fur Verbraucherschutz und Lebensmittelsicherheit* 6 (2): 233–236.
DfE. 2003. *Building Bulletin 87 - Guidelines for environmental design in schools.* Technical Report. Department for Education. http://science.cleapss.org.uk/Resource/Building-Bulletin-87-Guidelines-for-Environmental-Design-in-Schools.pdf.
DfE. 2014. *Building Bulletin 103 - Area guideines for mainstream schools.* Technical Report. Department for Education.
DfE. 2018. *Schools, Pupils, and Their Characteristics.* Technical Report June. London: Department for Education. https://www.gov.uk/government/statistics/schools-pupils-and-their-characteristics-january-2018.
Dias Pereira, Luísa, Daniela Raimondo, Stefano Paolo Corgnati, and Manuel Gameiro da Silva. 2014. "Energy consumption in schools – A review paper." *Renewable and Sustainable Energy Reviews* 40: 911–922. https://www.sciencedirect.com/science/article/pii/S1364032114006868#f0015.
Dodd, Nicholas, Elena Garbarin, and Miguel Gamas Caldas. 2016. *Green Public Procurement Criteria for Office Building Design, Construction and Management.* Technical Report. Brussels: European Union. https://ec.europa.eu/environment/gpp/pdf/report_gpp_office_buildings.pdf.
Fan, Yuzhi, Zhiming Zhong, and Xianzhou Zhang. 2011. "Determination of photosynthetic parameters Vcmax and Jmax for a C3 plant (spring hulless barley) at two altitudes on the Tibetan Plateau." *Agricultural and Forest Meteorology* 151 (12): 1481–1487. http://dx.doi.org/10.1016/j.agrformet.2011.06.004.
Farquhar, G. D., S. von Caemmerer, and J. A. Berry. 1980. "A biochemical model of photosynthetic CO2 assimilation in leaves of C3 species." *Planta* 149 (1): 78–90. http://link.springer.com/10.1007/BF00386231.
Ferentinos, K P, L D Albright, and D V Ramani. 2000. "Optimal Light Integral and Carbon Dioxide Concentration Combinations for Lettuce in Ventilated Greenhouses." *J. agric. Engng Res* 77 (3): 309–315. http://www.idealibrary.com.
Fischer, Günther, Francesco N. Tubiello, Harrij van Velthuizen, and David A. Wiberg. 2007. "Climate change impacts on irrigation water requirements: Effects of mitigation, 1990-2080." *Technological Forecasting and Social Change* 74 (7).
Fu, J. 2008. "Effects of different harvest start times on leafy vegetables (lettuce, pak choi and rocket) in a reaping and regrowth system." 1–103.
Galieni, A., F. Stagnari, S. Speca, and M. Pisante. 2016. "Leaf traits as indicators of limiting growing conditions for lettuce (Lactuca sativa)." *Annals of Applied Biology* 169 (3): 342–356. http://doi.wiley.com/10.1111/aab.12305.
Gent, Martin PN. 2012. "Composition of hydroponic lettuce: effect of time of day, plant size, and season." *Journal of the Science of Food and Agriculture* 92 (3): 542–550. http://doi.wiley.com/10.1002/jsfa.4604.
Goldstein, Benjamin, Michael Hauschild, John Fernández, and Morten Birkved. 2016. "Testing the environmental performance of urban agriculture as a food supply in northern climates." *Journal of Cleaner Production* 135: 984–994. https://www.sciencedirect.com/science/article/pii/S0959652616308952.
Gowri, K, D Winiarski, and R Jarnagin. 2009. *Infiltration Modeling Guidelines for Commercial*

Building Energy Analysis. Technical Report September.
Graamans, Luuk, Andy van den Dobbelsteen, Esther Meinen, and Cecilia Stanghellini. 2017. "Plant factories; crop transpiration and energy balance." *Agricultural Systems* 153: 138–147. http://linkinghub.elsevier.com/retrieve/pii/S0308521X16306515.
Gubb, C., T. Blanusa, A. Griffiths, and C. Pfrang. 2018. "Can houseplants improve indoor air quality by removing CO2 and increasing relative humidity?" *Air Quality, Atmosphere & Health* 11 (10): 1191–1201. http://link.springer.com/10.1007/s11869-018-0618-9.
Hong, Sung Min. 2015. "Benchmarking the energy performance of the UK non-domestic stock: a schools case study." PhD diss., UCL. http://discovery.ucl.ac.uk/1464471/1/SHONG_Thesis_Final_31Mar15.pdf.
Hunter, Mitchell C., Richard G. Smith, Meagan E. Schipanski, Lesley W. Atwood, and David A. Mortensen. 2017. "Agriculture in 2050: Recalibrating Targets for Sustainable Intensification." *BioScience* 67 (4): 386–391. https://academic.oup.com/bioscience/article/67/4/386/3016049.
Jans-Singh, Melanie. 2020. "meljsingh/EPfileCreator." Accessed 2021-03-16. https://github.com/meljsingh/EPfileCreator.
Jans-Singh, Melanie. 2021. "EECi/cosimulation." Accessed 2021-03-16. https://github.com/EECi/cosimulation.
Jans-Singh, Melanie, Kathryn Leeming, Ruchi Choudhary, and Mark Girolami. 2020. "Digital twin of an urban-integrated hydroponic farm." *Data-Centric Engineering* 1. https://www.cambridge.org/core.
Jans-Singh, Melanie Kiren, Rebecca Ward, and Ruchi Choudhary. 2020. "Co-simulation of a Rooftop Greenhouse and a School Building in London, UK." In *Proceedings of Building Simulation 2019: 16th Conference of IBPSA*, Vol. 16, 3, 3266–3273. IBPSA.
Jolliet, O., and B. J. Bailey. 1992. "The effect of climate on tomato transpiration in greenhouses: measurements and models comparison." *Agricultural and Forest Meteorology* 58 (1-2): 43–62.
Kozai, Toyoki. 2016. *Plant Factory - An Indoor Vertical Farming System for Efficient Quality Food Production*. Oxford, UK: Elsevier Inc.
Kulak, Michal, Anil Graves, and Julia Chatterton. 2013. "Reducing greenhouse gas emissions with urban agriculture: A Life Cycle Assessment perspective." *Landscape and Urban Planning* 111: 68–78.
Lee, J H, and E Heuvelink. 2003. "Simulation of leaf area development based on dry matter partitioning and specific leaf area for cut chrysanthemum." *Annals of botany* 91 (3): 319–27. http://www.ncbi.nlm.nih.gov/pubmed/12547684http://www.pubmedcentral.nih.gov/articlerender.fcgi?artid=PMC4244956.
Léveillé-Guillemette, Frederic, and Danielle Monfet. 2016. "Comparison of different mechanical systems models for a passive solar greenhouse with two thermal zones." *Proceedings froms BSO16: USA* .
Menberg, Kathrin, Yeonsook Heo, and Ruchi Choudhary. 2016. "Sensitivity analysis methods for building energy models: Comparing computational costs and extractable information." *Energy and Buildings* 133: 433–445. https://linkinghub.elsevier.com/retrieve/pii/S0378778816311112.
Monteith, John L., and M. H. Unsworth. 2008. "Microclimatology of Radiation: (iii) Interception by Plant Canopies and Animal Coats." In *Principles of environmental physics*, 3rd ed., Chap. 8, 418. Elsevier.
Muñoz-Liesa, Joan, Mohammad Royapoor, Elisa López-Capel, Eva Cuerva, Martí Rufí-Salís, Santiago Gassó-Domingo, and Alejandro Josa. 2020. "Quantifying energy symbiosis of building-integrated agriculture in a mediterranean rooftop greenhouse." *Renewable Energy* 156: 696–709.
Mysen, M, and P G Schild. 2009. *Recommendations on Specific Fan Power and Fan System Efficiency - Technical Note AIVC 65*. Technical Report. Leuwen: International Energy Agency. https://www.aivc.org/sites/default/files/members_area/medias/pdf/Technotes/TN65_SpecificFanPower.pdf.

Nadal, Ana, Pere Llorach-Massana, Eva Cuerva, Elisa López-Capel, Juan Ignacio Montero, Alejandro Josa, Joan Rieradevall, and Mohammad Royapoor. 2017. "Building-integrated rooftop greenhouses: An energy and environmental assessment in the mediterranean context." *Applied Energy* 187: 338–351. http://www.sciencedirect.com/science/article/pii/S0306261916316361.

Nadal, Ana, Oriol Pons, Eva Cuerva, Joan Rieradevall, and Alejandro Josa. 2018. "Rooftop greenhouses in educational centers: A sustainability assessment of urban agriculture in compact cities." *Science of The Total Environment* 626: 1319–1331. https://www.sciencedirect.com/science/article/pii/S0048969718302328?via%3Dihub#bb0140.

New York Sun Works. 2020. "Impact — New York Sun Works." https://nysunworks.org/about/impact/.

Nguyen, Anh Tuan, and Sigrid Reiter. 2015. "A performance comparison of sensitivity analysis methods for building energy models." *Building Simulation* 8 (6): 651–664. https://link.springer.com/article/10.1007/s12273-015-0245-4.

Orsini, Francesco, Remi Kahane, Remi Nono-Womdim, and Giorgio Gianquinto. 2013. "Urban agriculture in the developing world: A review." *Agronomy for Sustainable Development* 33 (4): 695–720. http://link.springer.com/10.1007/s13593-013-0143-z.

Park, Dae-Heon, and Jang-Woo Park. 2011. "Wireless Sensor Network-Based Greenhouse Environment Monitoring and Automatic Control System for Dew Condensation Prevention." *Sensors* 11 (12): 3640–3651. http://www.mdpi.com/1424-8220/11/4/3640/.

Pieters, J. G., and J. M. Deltour. 1997. "Performances of greenhouses with the presence of condensation on cladding materials." *Journal of Agricultural and Engineering Research* 68 (2): 125–137.

Poore, J., and T. Nemecek. 2018. "Reducing food's environmental impacts through producers and consumers." *Science* 360 (6392).

Railio, Jorma, and Pekka Mäkinen. 2007. "SPECIFIC FAN POWER - a tool for better performance of air handling systems." In *Proceedings of Clima 2007 WellBeing Indoors*, Helsinki. http://www.irbnet.de/daten/iconda/CIB7187.pdf.

Roser, Max, and Hannah Ritchie. 2019. "Land Use." https://ourworldindata.org/land-use.

Santosh, Philip. 2019. "eppy: scripting language for E+, Energyplus." https://github.com/santoshphilip/eppy.

Sanyé-Mengual, Esther, Jordi Oliver-Solà, Juan Ignacio Montero, and Joan Rieradevall. 2015. "An environmental and economic life cycle assessment of rooftop greenhouse (RTG) implementation in Barcelona, Spain. Assessing new forms of urban agriculture from the greenhouse structure to the final product level." *International Journal of Life Cycle Assessment* 20 (3): 350–366.

Schoen, Victoria, and Tim Lang. 2016. *Horticulture in the UK: potential for meeting dietary guideline demands*. Technical Report.

Siegner, Alana, Jennifer Sowerwine, and Charisma Acey. 2018. "Does Urban Agriculture Improve Food Security? Examining the Nexus of Food Access and Distribution of Urban Produced Foods in the United States: A Systematic Review." *Sustainability* 10 (9): 2988. http://www.mdpi.com/2071-1050/10/9/2988.

Slamet, Widyati, Endang Dwi Purbajanti, Adriani Darmawati, and Eny Fuskhah. 2017. "Leaf area index, chlorophyll, photosynthesis rate of lettuce (Lactuca sativa L) under N-organic fertilizer." *Indian Journal of Agricultural Research* 51 (4): 365–369. https://pdfs.semanticscholar.org/6c2c/dbb1eb7696139e8647f8bd645661a7eb1d4e.pdf.

Specht, Kathrin, Rosemarie Siebert, Ina Hartmann, Ulf B. Freisinger, Magdalena Sawicka, Armin Werner, Susanne Thomaier, Dietrich Henckel, Heike Walk, and Axel Dierich. 2013. "Urban agriculture of the future: an overview of sustainability aspects of food production in and on buildings." *Agriculture and Human Values* 1–19.

Stanghellini, C., and W. Th m. van Meurs. 1992. "Environmental control of greenhouse crop transpiration." *Journal of Agricultural Engineering Research* 51 (C): 297–311.

Tei, F, A. Scaife, and D. P. Aikman. 1996. "Growth of Lettuce, Onion, and Red Beet. 1. Growth

Analysis, Light Interception, and Radiation Use Efficiency." *Annals of Botany* 78 (5): 633–643. https://academic.oup.com/aob/article-lookup/doi/10.1006/anbo.1996.0171.

The Carbon Trust. 2012. *CT009 Agriculture and Horticulture - Sector Overview.* Technical Report. London. https://www.carbontrust.com/media/39180/ctv009_agriculture_and_horticulture.pdf.

The GeoInformation Group. 2017. *UKMap User Guide.* Technical Report. Cambridge: Verisk Analytics.

The Mathworks Inc. 2016. *MATLAB version r2016a.* Technical Report. Natick, Massachusetts.

Thomaier, Susanne, Kathrin Specht, Dietrich Henckel, Axel Dierich, Rosemarie Siebert, Ulf B. Freisinger, and Magdalena Sawicka. 2015. "Farming in and on urban buildings: Present practice and specific novelties of Zero-Acreage Farming (ZFarming)." *Renewable Agriculture and Food Systems* 30 (01): 43–54. http://www.journals.cambridge.org/abstract_S1742170514000143.

Thompson, Helen C, and Robert W Langhans. 1998. "Shoot and root temperature effects on lettuce growth in a floating hydroponic system." *Journal of the American Society for Horticultural Science* 123 (3): 361–364. http://journal.ashspublications.org/content/123/3/361.full.pdf.

Tian, Wei. 2013. "A review of sensitivity analysis methods in building energy analysis." *Renewable and Sustainable Energy Reviews* 20: 411–419.

Tian, Wei, and R. Choudhary. 2012. "A probabilistic energy model for non-domestic building sectors applied to analysis of school buildings in greater London." *Energy and Buildings* 54: 1–11. https://www.sciencedirect.com/science/article/pii/S0378778812003544#fig0005.

Tibbitts, T W, and G Bottenberg. 1976. "Growth of lettuce (Lactuca sativa) under controlled humidity levels." *Journal of the American Society for Horticultural Science* 101 (1): 70–73. https://www.researchgate.net/publication/233860952_Growth_of_lettuce_Lactuca_sativa_under_controlled_humidity_levels.

United Nations. 2019. *World Urbanization Prospects: The 2018 Revision.* Technical Report. New York: United Nations: Department of Economic and Social Affairs, Population Division.

USDA. 2017. "Romaine and leaf lettuces almost as popular as head lettuce." https://www.ers.usda.gov/data-products/chart-gallery/gallery/chart-detail/?chartId=93321.

Van Iersel, M. W. 2003. "Carbon use efficiency depends on growth respiration, maintenance respiration, and relative growth rate. A case study with lettuce." *Plant, Cell and Environment* 26 (9): 1441–1449.

Vanthoor, B H E. 2011. "A model-based greenhouse design method." PhD diss., Wageningen University.

Von Caemmerer, Susanne. 2013. "Steady-state models of photosynthesis." *Plant, Cell and Environment* .

Walker, Anthony P., Andrew P. Beckerman, Lianhong Gu, Jens Kattge, Lucas A. Cernusak, Tomas F. Domingues, Joanna C. Scales, Georg Wohlfahrt, Stan D. Wullschleger, and F. Ian Woodward. 2014. "The relationship of leaf photosynthetic traits - Vcmax and Jmax - to leaf nitrogen, leaf phosphorus, and specific leaf area: A meta-analysis and modeling study." *Ecology and Evolution* 4 (16): 3218–3235.

Ward, R., R. Choudhary, C. Cundy, G. Johnson, and A. McRobie. 2015. "Simulation of plants in buildings; incorporating plant-air interactions in building energy simulation." In *14th International Conference of IBPSA - Building Simulation 2015, BS 2015, Conference Proceedings*, .

Ward, R. M., and R. Choudhary. 2014. "A bottom-up energy analysis across a diverse urban building portfolio: Retrofits for the buildings at the Royal Botanic Gardens, Kew, UK." *Building and Environment* 74: 132–148.

Ward, Rebecca, Melanie Jans-Singh, and Ruchi Choudhary. 2018. "Quantifying the Environmental and Energy Benefits of Food Growth in the Urban Environment." In *Smart Plant Factory - The Next Generation Indoor Vertical Farms*, edited by Toyoki Kozai, Chap. 17.

Chiba, Japan: Springer.
Watson, J A, C Gómez, D E Buffington, R A Bucklin, R W Henley, and D B Mcconnell. 2019. *AE-10 Greenhouse Ventilation*. Technical Report. Institute of Food and Agricultural Sciences. https://edis.